

1
2
3
4 1 **The Impact of Inter-flood Duration on Non-Cohesive**
5
6 2 **Sediment Bed Stability**
7
8
9
10 3
11 4
12
13

14 5 Annie Ockelford^{1*}, Stephen Woodcock², Heather Haynes³
15
16 6
17
18 7
19
20

21 81. *Centre for Aquatic Environments, University of Brighton, Brighton, BN2 4GJ Email*
22

23 9 (a.ockelford@brighton.ac.uk) * corresponding author
24
25
26 10
27

28 112. *School of Mathematical Sciences University of Technology Sydney, Sydney,*
29

30 12 *Australia NSW 2007*
31
32
33 13
34 14
35

36 153. *Water Academy, Heriot-Watt University, Edinburgh, EH14 4 AS*
37
38
39 16
40
41 17
42
43 18
44

45 19 **Short Title: Inter- flood duration and bed stability**
46
47
48
49
50
51
52
53
54
55
56
57
58
59
60

ABSTRACT

Limited field and flume data suggests that both uniform and graded beds appear to progressively stabilise when subjected to inter flood flows as characterised by the absence of active bedload transport. Previous work has shown that the degree of bed stabilization scales with duration of inter-flood flow, however, the sensitivity of this response to bed surface grain size distribution has not been explored. This paper presents the first detailed comparison of the dependence of graded bed stability on inter-flood flow duration. Sixty discrete experiments, including repetitions, were undertaken using three grain size distributions of identical D_{50} (4.8mm); near-uniform ($\sigma_g = 1.13$), unimodal ($\sigma_g = 1.63$) and bimodal ($\sigma_g = 2.08$). Each bed was conditioned for between 0 (benchmark) and 960 minutes by an antecedent shear stress below the entrainment threshold of the bed (τ_{c50}^*). The degree of bed stabilisation was determined by measuring changes to critical entrainment thresholds and bedload flux characteristics.

Results show that (i) increasing inter-flood duration from 0 to 960 minutes increases the average threshold shear stress of the D_{50} by up to 18%; (ii) bedload transport rates were reduced by up to 90% as inter-flood duration increased from 0 to 960 minutes; (iii) the rate of response to changes in inter-flood duration in both critical shear stress and bedload transport rate is nonlinear and is inversely proportional to antecedent duration; (iv) there is a grade dependent response to changes in critical shear stress where the magnitude of response in uniform beds is up to twice that of the graded beds; and (v) there is a grade dependent response to changes in bedload transport rate where the bimodal bed is most responsive in terms of the magnitude of change. These advances underpin the development of more accurate predictions of both entrainment thresholds and bedload flux timing and magnitude, as well as having implications for the management of environmental flow design.

Key Words; inter-flood duration, entrainment threshold, bedload flux, grain size distribution

1. INTRODUCTION

In non-cohesive sediment beds it is traditionally assumed that bed structure and hence, resistance to entrainment, is only capable of being modified when the applied shear stress exceeds the threshold for incipient motion (Gomez, 1983; Reid *et al.*, 1985; Church *et al.*, 1998; Powell *et al.*, 1999). This theory suggests that low, inter-flood flow periods will have no effect on bed stability and bed restructuring will only occur during flood events which result in active bedload transport modifying surface stability. However, field (Reid and Frostick, 1984; Reid *et al.*, 1985; Masteller *et al.*, 2019) and flume (Paphitis and Collins, 2005; Monteith and Pender, 2005; Haynes and Pender, 2007; Ockelford and Haynes, 2012; Masteller and Finnegan, 2017) data suggests that both uniform and graded beds appear to progressively stabilise even when subjected to the low shear stresses experienced during inter-flood flow periods.

Given that most commonly used sediment transport formulae use empirical relationships between bedload transport rate and flow intensity (Meyer-Peter & Müller, 1948; Bagnold, 1980; Ashmore, 1988; Parker, 1990; Zhang and McConnachie, 1994; Hassan and Woodsmith, 2004; Barry *et al.*, 2008; Recking, 2010), and tend to rely on the assumption that a single critical value of shear stress can be used to predict the onset of motion (e.g., Meyer-Peter and Müller, 1948; Engelund and Fredsøe 1975; Wong and Parker, 2006) small errors in shear stress estimations can cause significant errors in bedload transport rate estimations (Buffington and Montgomery, 1997; Recking *et al.*, 2012; Schneider *et al.*, 2015). Thus, understanding how periods of prolonged, inter-flood flow, affect the onset of

1
2
3 80 motion could be used to improve the predictive capability of certain sediment
4
5 81 transport formulae.

6
7
8 82 These periods of antecedent flow have been termed 'stress history', which describes
9
10 83 a time-dependent 'memory' effect, where the combined effect of the duration and
11
12 84 magnitude of antecedent flows influences entrainment thresholds and bedload flux.

13
14 85 This typically describes the low flow period between significant sediment-transporting
15
16 86 events, where sediment transport rates are negligible or of very low exhibit low
17
18 87 partial-transport conditions. Field data from the non-cohesive graded river bed of
19
20 88 Turkey Brook showed entrainment thresholds up to three times higher during
21
22 89 isolated flood events compared to floods which occurred with a shorter return period.

23
24 90 Although not specifically quantified, it was hypothesised that shorter inter-flood
25
26 91 durations left the bed material comparatively loose and more susceptible to
27
28 92 entrainment in the subsequent flood event. As inter-flood duration increased more
29
30 93 advanced bed re-structuring left the bed more resistant to entrainment with lower
31
32 94 bedload transport rates in the subsequent flood (Reid and Frostick, 1984; Reid *et al.*,
33
34 95 1985). Pfeiffer and Finnegan (2018) observed that regional trends linked with
35
36 96 hydrological regime controlled the bed surface mobility discussed in terms of the
37
38 97 proportion of time a channel is above the conditions of threshold mobility; rivers
39
40 98 characterised as having longer periods of high flow during snowmelt periods have
41
42 99 higher relative mobility as compared to those characterised by abrupt brief flood
43
44 100 events with longer inter- flood durations.

45
46 101
47
48 102 Direct laboratory evidence provides support for the importance of stress history
49
50 103 effects. Paphitis and Collins (2005) studied the entrainment threshold for uniform
51
52 104 sand beds subjected to antecedent flow durations of up to 120 minutes. Their data
53
54
55
56
57
58
59
60

1
2
3 105 indicated the critical shear stress increased by up to 61% following exposure to
4
5 106 prolonged durations of antecedent flow. Similarly, Monteith and Pender (2005) and
6
7 107 Haynes and Pender (2007) exposed a bimodal sand-gravel mixture to increasing
8
9 108 antecedent conditioning flow durations; up to a 48% increase in critical bed shear
10
11 109 stress was noted as antecedent duration was increased from 0 to 5760 minutes.
12
13 110 Bedload flux has also been shown to be responsive to the duration of antecedent
14
15 111 flow where the same authors noted a 38% reduction in total bedload flux as
16
17 112 antecedent duration was increased. Using a unimodal gravel distribution and
18
19 113 conditioning flow periods between 1 and 200 minutes Masteller and Finnegan (2017)
20
21 114 noted an 86% reduction in bedload flux. This reduction was characterised by a
22
23 115 linear reduction in cumulative bedload flux in the period following antecedent flows
24
25 116 which was attributed to the re-organisation of the highest protruding grains on the
26
27 117 bed surface. However, they note the antecedent durations they used needed to be
28
29 118 increased to more accurately constrain the bedload flux relationships with
30
31 119 antecedent flow. This link between changes in bedload transport rate and bed
32
33 120 topography in response to periods of sub threshold flow was also quantified by
34
35 121 Ockelford and Haynes (2012). Using the same distributions and antecedent time
36
37 122 periods as reported herein, they quantified changes to bed topography pre and post
38
39 123 application of sub threshold flows. They noted that stress history response of the
40
41 124 bed surface was grade specific, where bed roughness decreased in uniform beds
42
43 125 but increased in graded beds in response to the application of the antecedent flow
44
45 126 period. This was reasoned to be due to the uniform bed having larger pore spaces
46
47 127 and a greater freedom to rearrange (Ockelford and Haynes, 2012). Grade dependent
48
49 128 bed stability, related to both entrainment thresholds and bedload flux, has also been
50
51 129 linked to the proportion of fines within a distribution controlling its stability response.
52
53
54
55
56
57
58
59
60

1
2
3 130 Frostick et al. (1984) suggested that past floods control the proportion of fine
4
5 131 sediment infiltrated into the coarser matrix, changing the sediment transport
6
7 132 conditions of future floods. Marquis and Roy (2012) noted that bed
8
9
10 133 dilation/contraction caused by fine sediment infiltration or winnowing in a gravel
11
12 134 framework related to bed conditions left by previous events, highlighting the role of
13
14
15 135 flood history on sediment transport in gravel-bed rivers.
16
17 136

18
19 137 Research to date has therefore shown that when beds are exposed to periods of
20
21 138 antecedent flow they appear to stabilise. This has been shown as both a change to
22
23 139 the critical shear stress and the magnitude and timing of bedload flux. However, the
24
25 140 differences in the methodologies used, the different timeframes employed and the
26
27 141 single grades investigated within the small body of previous stress history literature
28
29 142 precludes direct comparison of data. To date no studies have directly compared the
30
31 143 response of both entrainment threshold and bedload flux within the same set of
32
33 144 experiments and thus it has been difficult to explicitly link one with the other.
34
35
36
37
38 145

39
40 146 This paper is the first to explore the relationship between the evolving critical shear
41
42 147 stress and bedload flux characteristics in response to varying inter-flood durations in
43
44 148 gravel bed rivers. We present a series of flume experiments that directly compares
45
46 149 three sediment grades of equivalent D_{50} and examines their response to changing
47
48 150 inter-flood duration. In so doing, we highlight a grade dependent response to inter-
49
50 151 flood duration which has implications for the deterministic definition of entrainment
51
52 152 and hence accurate prediction of the transition between river bed stability and
53
54 153 instability.
55
56
57
58 154
59
60

2. Methodology

2.1 Experimental Procedure

Experiments were performed within a flow-recirculating, tilting flume (13m long × 1.8m wide × 0.35m deep), set to a bed slope of 1/200. Within the flume, a 2m length of coarse, immobile sediment located immediately downstream of the inlet (to help prevent scour and induce fully turbulent flow) preceded an 8m test length of mobile test sediments that was screeded to a 60mm depth (~4D_{max} where D_{max} is the maximum grain size of 16mm). Due to the low transport rates within experiments, no notable scour or water surface perturbations were discernible at the immobile-mobile bed transition.

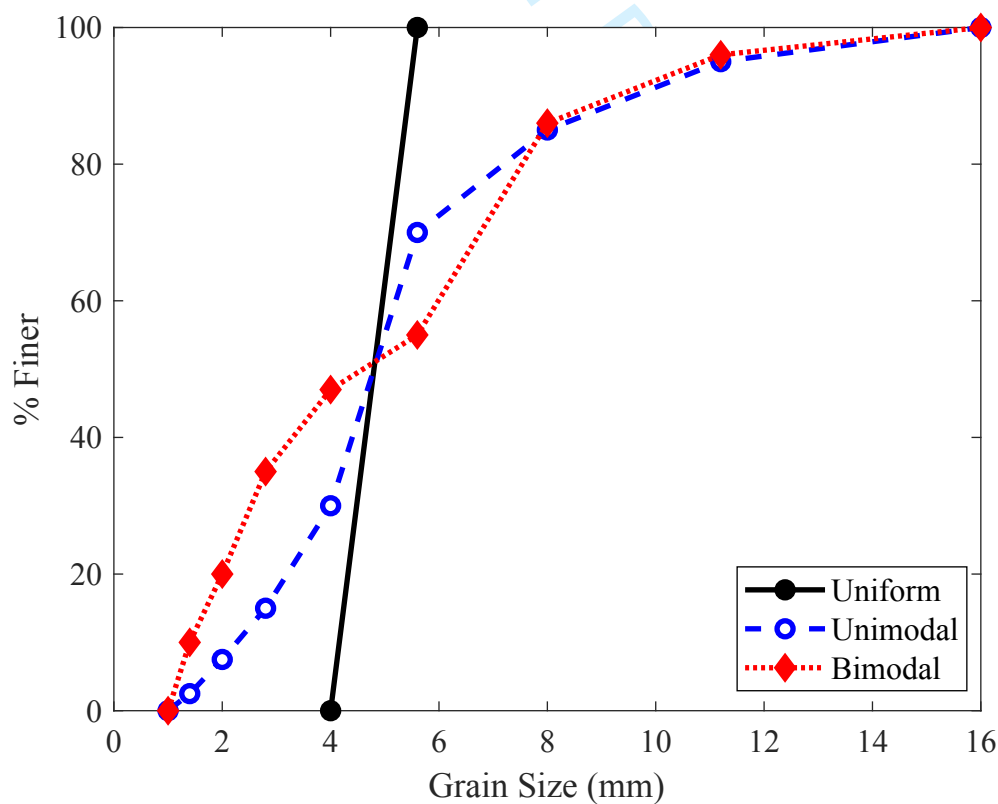
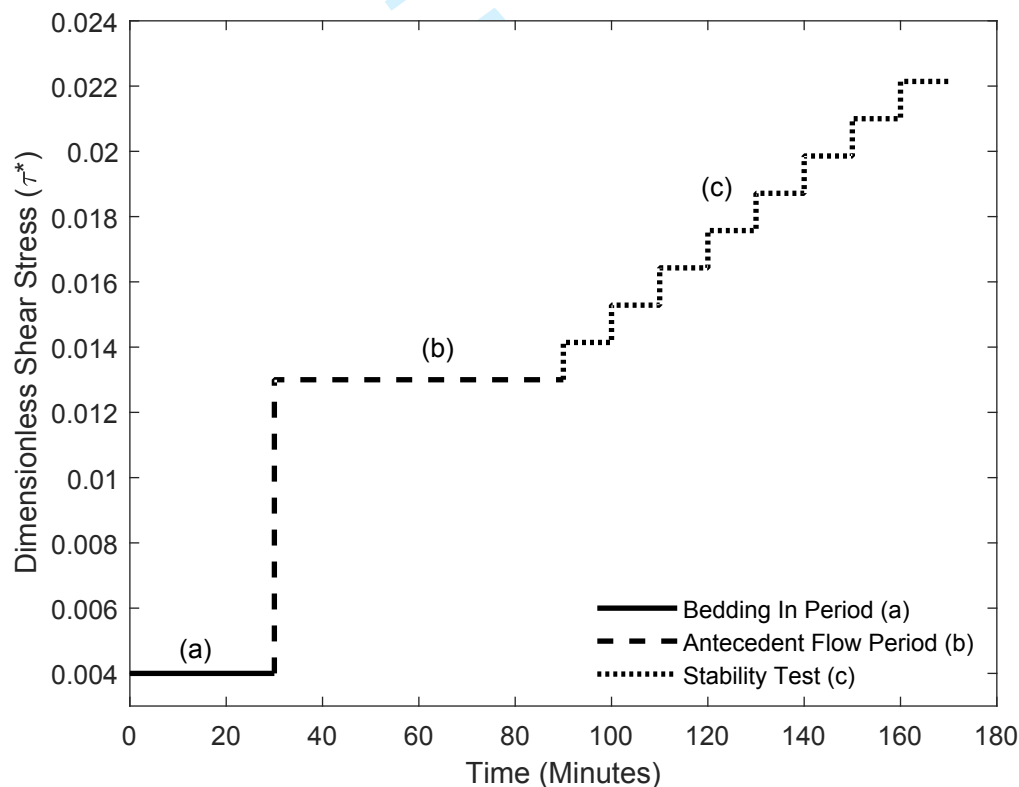


Figure 1: Grain size distribution for the three test sediment grades. The is calculated according to $\sigma_g = (D_{84}/D_{16})^{0.5}$

1
2
3
4 170 Three grain size distributions of identical D_{50} (4.8mm); near-uniform ($\sigma_g = 1.13$),
5 171 unimodal ($\sigma_g = 1.63$) and bimodal ($\sigma_g = 2.08$) were generated using natural sub-
6 172 rounded sand and gravel ranging from 1 to 16mm in diameter (Krumbein, 1941) with
7 173 a density of 2560kg/m^3 (Figure 1). Sediments were dry sieved to obtain eight size
8 174 fractions at standard $\frac{1}{2}$ phi intervals and then recombined into the desired
9 175 distributions with the D_{50} and D_{84} fractions painted for identification purposes (Table
10 176 1). During each experiment three phases were run: (a) an initial bedding in period;
11 177 (b) an antecedent flow period and; (c) a stability test (Figure 2).
12 178



179
180 **Figure 2:** Sample experimental hydrograph detailing the three stages of the
181 experiment: (a) an initial bedding in period run for 30 minutes at $\tau^* \sim 0.004$; (b) an
182 antecedent flow period run at τ^*_{c50} for 0, 60, 120, 240 or 960 minutes; and (c) a
183 stability test run until τ^*_{c50} is reached. The dimensionless shear stress values for
184 each phase of each experiment are given in Table 1 with the example here given for
185 the uniform bed exposed to 60 minutes of antecedent flow.
186

1
2
3 187 The bedding-in period employed a flow depth of 10 mm ($\tau^* \sim 0.004$) for 30 minutes
4
5 188 duration; this was designed to remove any air pockets or unstable grains generated
6
7 189 within the bed screeding process. In line with the methodology of Ockelford and
8
9
10 190 Haynes (2012), flow was then increased to apply a shear stress equating to 50% of
11
12 191 the critical threshold for entrainment of the median grain size (τ^*_{c50}) benchmarked for
13
14 192 when no inter- flood flow was applied (i.e. 0 minutes of antecedent flow applied with
15
16
17 193 τ^*_{c50} values under these conditions given in Table 1). This was calculated using the
18
19 194 quantitative visual definition of threshold of Neill and Yalin (1969) in which the
20
21 195 number of grain detachments (m_i) from a given bed area (A) over a given time (t)
22
23 196 were counted, and the threshold determined according to Equation 1.

$$m_i = \frac{\varepsilon A t}{\sqrt{\frac{\rho D^5}{(\rho_s - \rho)g}}} \quad (\text{Eq. 1})$$

24
25
26 197
27
28
29
30
31
32 198 where a lower limit of ε was defined by Neill and Yalin as 1.0×10^{-6} , and ρ_s and ρ
33
34 199 are the sediment and fluid density respectively. The observation area (A) was
35
36 200 located in the centre of the flume 11m downstream of the inlet, this was sized 0.04m^2
37
38 201 and the time of observation (t) was set 180 seconds. Once the threshold number of
39
40 202 detachments was reached critical shear stress was estimated from the depth-slope
41
42 203 product corrected for the roughness effects of both the side walls and the bed
43
44 204 according to Manning's n and derived according to the methodology followed by
45
46 205 Monteith and Pender (2005). This second flow stage constituted the 'antecedent'
47
48 206 period, with applied dimensionless shear stress values of 0.016, 0.020, 0.019 of the
49
50 207 D_{50} for the uniform, unimodal and bimodal beds respectively. Antecedent flows were
51
52 208 applied for either 0 (benchmark), 60, 120, 240 or 960 minutes. No sediment
53
54 209 entrainment was observed during this period and quasi-uniform sub-critical flow was
55
56 210 maintained throughout.

1
2
3 211
4
5 212 A final flow stage, the 'stability test' was then applied in steps of increasing shear
6
7 213 stress. The shear stress was increased by approximately 0.24 Nm^{-2} during each
8
9 214 step which equated to a 5mm flow depth increase or a dimensionless shear stress
10
11 215 increase of 0.003 at each step. The stability test was run until the threshold criterion
12
13 216 derived from Neill and Yalin were satisfied. Flow steps were 600 second increments
14
15 217 which was sufficient to allow flow stabilisation and visual assessment, using the Yalin
16
17 218 criterion, of whether or not the new entrainment threshold had been reached. Since
18
19 219 the critical shear stress varied according to both grain size distribution and
20
21 220 antecedent duration the applied the stability test duration ranged from 50 to 80
22
23 221 minutes (Table 1). Each of these experiments was repeated three times. Reported
24
25 222 critical dimensionless shear stress values were calculated from an average of these
26
27 223 three experimental runs (first three experiments detailed for each experiment
28
29 224 combination in Table 1).

30
31
32
33
34
35 225
36
37 226 Bedload data was collected from one additional, separate run for each of the
38
39 227 experiment combinations (the fourth experiment detailed in Table 1). During this
40
41 228 separate experiment, bedload data was collected at each step of the stability test,
42
43 229 where each step was 600 seconds long as per the entrainment threshold analysis
44
45 230 experiments. Flow was stopped once the critical entrainment threshold, as calculated
46
47 231 from the three previous entrainment threshold experiments, was reached. Mobile
48
49 232 sediment was collected in a trap located 12m downstream of the flume inlet with
50
51 233 sampling slot 75mm wide and of streamwise length 150mm. Bedload was collected
52
53 234 at each step of the stability test and collected material was air dried overnight and
54
55 235 sieved the individual size fractions. Bedload flux calculations were both integrated
56
57
58
59
60

1
2
3 236 over the entire stability test (Figure 4), as well as over the individual steps of the
4
5 237 stability test (Figure 5). Fractional transport rates were calculated from the total
6
7 238 bedload collected during the final step of the stability test which represents the
8
9 239 critical threshold conditions of the D_{50} (Figure 6). Sediment was not recirculated or
10
11 240 fed into the flume during the individual experiments but was returned to the flume
12
13 241 between experiments. The bed was fully mixed and re-screeded between
14
15 242 experiments to preclude inheritance effects from previous experiments. A total of 60
16
17 243 discrete experiments (including repeats) were undertaken (Table 1).
18
19
20
21
22 244

245 **2.2 Experimental Uncertainty**

246
247 The experiments presented herein allow for the quantification of inter-flood duration
248 effects on bed stability via the direct measurement of critical shear stress and
249 bedload flux. However, methodological issues can introduce uncertainty into these
250 measurements including: (i) inaccurate screeding such that the grain size distribution
251 of the starting bed surface distribution varies between the different experiments; and,
252 (ii) issues of subjectivity surrounding the derivation of threshold according to the
253 Yalin Criterion. Given the D_{50} and D_{84} fractions were coloured, the effects of
254 screeding were analysed using bed surface photographs taken after the initial
255 screed. The numbers of grains belonging to each fraction were counted and the
256 $D_{50}:D_{84}$ ratio calculated. Results indicate $\leq 1.5\%$ variability between the screeded
257 beds, providing confidence that any differences in bed composition stem solely from
258 the active processes pertaining to the experiment itself. The subjectivity in use of the
259 Yalin Criterion was minimised via data collection using a single operator.
260 Comparison of multiple repeats of runs shows an average variability of 4.8% in terms

1
2
3 261 of the calculated average critical dimensionless shear stress (Table 1; this is in line
4
5 262 with experimental error of similar laboratory studies (Piedra and Haynes, 2011). The
6
7 263 highest variability is typically associated with the shortest antecedent flow durations
8
9 264 where there is the greatest rate of change in the shear stress. As such the variability
10
11 265 in the average critical shear stress is never larger than the absolute change in shear
12
13 266 stress and does not therefore change the relationship between critical shear stress
14
15 267 and antecedent duration.
16
17
18
19
20
21
22

23 269 **3. RESULTS**

24 25 270 26 27 28 271 **3.1 Inter-flood duration effects on entrainment threshold**

29
30
31 272
32
33 273 The relationship between entrainment threshold and inter-flood duration is
34
35 274 summarised by Figure 3. Under benchmark conditions with no inter-flood flow
36
37 275 applied critical dimensionless shear stress shows a hierarchy to bed stability:
38
39 276 unimodal (0.039): bimodal (0.033); uniform (0.031). After the application of the
40
41 277 antecedent period there is a positive correlation with between the antecedent
42
43 278 duration and dimensionless critical shear stress for all three grain size distributions.
44
45 279 However, the magnitude of the increase in critical shear stress compared to the
46
47 280 benchmark experiments is grade specific: near uniform (+18%) > bimodal (+12%)>
48
49 281 unimodal (+9%).
50
51
52
53
54 282

55
56 283 There is also an apparent difference between the rate of change in critical
57
58 284 dimensionless shear stress in response to the applied antecedent flow. In order to
59
60

1
2
3 285 quantify the rate of change, parametric curves have been applied to the entrainment
4
5 286 threshold data. The fitted curves used herein are distinct from the only other
6
7 287 previous attempt to model growth of Paphitis and Collins (2005) whose 'exposure
8
9 288 correction' described logarithmic growth of their entrainment threshold function in
10
11 289 response to increasing inter-flood durations. Whilst their mathematical form correctly
12
13 290 describes progressive slowing of growth of inter-flood duration effects over
14
15 291 lengthening timeframes, it holds an implicit assumption of unbounded growth as time
16
17 292 tends towards infinity; i.e. if left for a prolonged period of time, the bed will keep
18
19 293 gaining in stability. As a sediment bed cannot become infinitely stressed, such a
20
21 294 logarithmic description is inaccurate; rather, it must tend to a limiting value
22
23 295 commensurate with the stability maxima of the bed. Two alternative mathematical
24
25 296 forms are, therefore, considered which both start and tend to finite values. Such
26
27 297 parametric curves have been used in ecological modelling (Noy-Meir, 1978) and in
28
29 298 enzyme kinetics (Michaelis and Menten, 1913) to describe similar rates of change
30
31 299 characterised by an initially linear increases which slows asymptotically towards
32
33 300 some maximal value. The first is described by Equation 2 below with the fit
34
35 301 parameters given in Table 2.

$$302 \quad \tau_c = \tau_{\max} - (\tau_{\max} - \tau_0)e^{-kt} \quad (\text{Eq. 2})$$

303 where τ_c represents the critical dimensionless shear stress, t represents antecedent
304 duration (minutes), τ_{\max} is the maximal critical dimensionless shear stress, τ_0 gives the
305 initial critical dimensionless shear stress and k is a free parameter (units mins⁻¹)
306 controlling how quickly τ_c increases. This model assumes that there is a maximum
307 possible stress and that the difference between the current stress and the maximum
308 stress decreases exponentially.

309

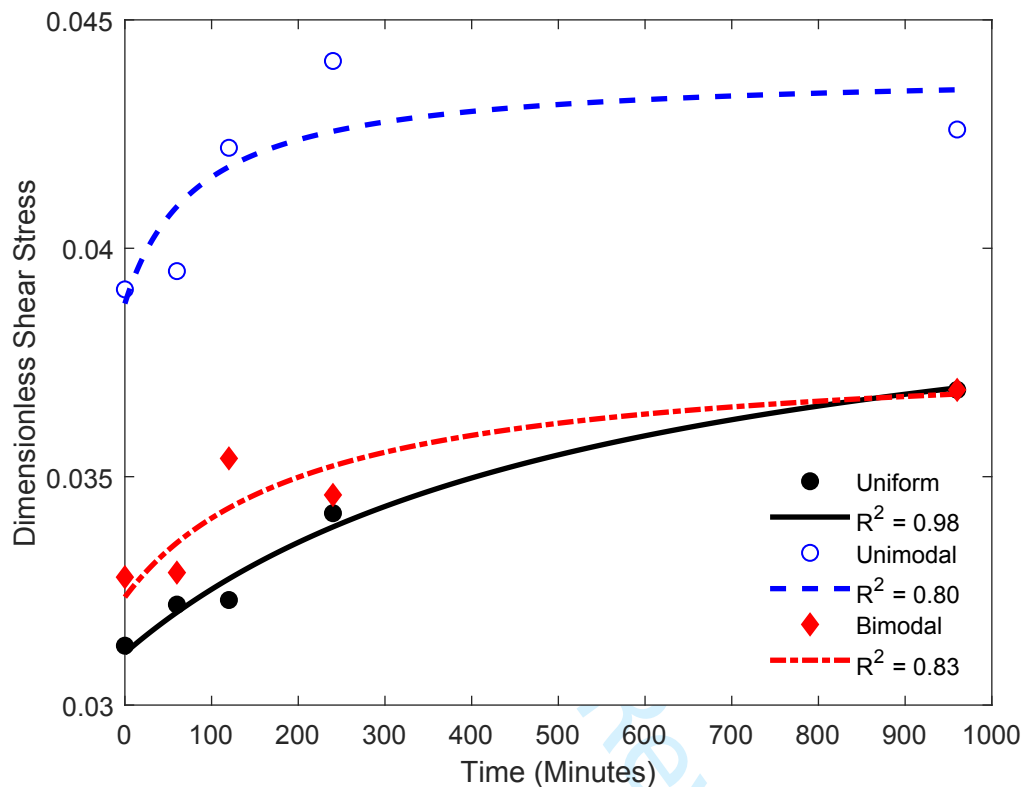
1
2
3 310 The alternative model is described by Equation 3 with the fit parameters given in
4
5 311 Table 3:

$$312 \quad \tau_c = \tau_0 + t \left(\frac{\tau_{\max} - \tau_0}{t + t_{1/2}} \right) \quad (\text{Eq. 3})$$

13
14 313 where τ_c represents the critical dimensionless shear stress, t represents antecedent
15
16 314 duration (minutes), τ_{\max} is the maximal critical dimensionless shear stress, τ_0 gives
17
18 315 the initial critical dimensionless shear stress and $t_{1/2}$ is the time until half the maximal
19
20 316 shear stress has been reached (minutes). Thus, both Eq. 2 and Eq. 3 assume that
21
22 317 when $t = 0$ then $\tau_c = \tau_0$; when $t \rightarrow \infty$ then $\tau_c \rightarrow \tau_{\max}$. The best fit models were selected
23
24 318 based on minimising the squared error between the model and the observed data
25
26 319 points.

27
28
29
30
31 320
32
33 321 The R^2 , RSME and SSE data are similar for both model fits and describe the data
34
35 322 well (Tables 2 and 3); the fits derived from Equation 2 are shown in Figure 3 given
36
37 323 the greater model skill and are described below. As reported, the parametric curve
38
39 324 indicates the uniform bed to be the most responsive to the effects of antecedent flow
40
41 325 duration and the unimodal the least (Figure 3, Table 2). The model indicates that the
42
43 326 rate of increase in critical dimensionless shear stress in response to increased inter-
44
45 327 flood duration varies between distributions as indicated by the time to half-life. The
46
47 328 unimodal bed has the greatest rate of response to inter-flood flows where the time to
48
49 329 half-life occurs within 74 minutes. This is compared to the bimodal and uniform beds
50
51 330 which take approximately twice and three times as long respectively. However, both
52
53 331 models predict that if antecedent duration continues to increase there will be very
54
55
56
57
58
59
60

332 little further stability gains; there will be a further percentage increase in stability of
 333 5%, 2% and 1% for the uniform, unimodal and bimodal beds respectively.



336 **Figure 3:** The relationship between antecedent duration, average critical
 337 dimensionless shear stress and grain size distribution with fits plotted derived
 338 according to Equation 2.

341 3.2 Inter-flood duration effects on bedload transport rate and characteristics

343 Both the magnitude and rate of response to the applied antecedent flow is grade
 344 dependent. Given most sediment transport formulae rely on the use of a single
 345 critical value of shear stress (e.g., Meyer-Peter and Müller, 1948; Engelund and
 346 Fredsøe 1975; Wong and Parker, 2006) understanding how periods of prolonged,
 347 inter-flood flow affect the onset of motion could be used to reduce the uncertainty in

these. Previous research has linked changes to entrainment thresholds in response to periods of sub threshold flow with changes to the magnitude and rate of bedload flux (Haynes and Pender, 2007; Masteller and Finnegan, 2017). As such, transport rate and fractional analysis of the bedload transported during the stability test was undertaken to provide insight into the links between changes to entrainment thresholds and the subsequent bedload flux characteristics.

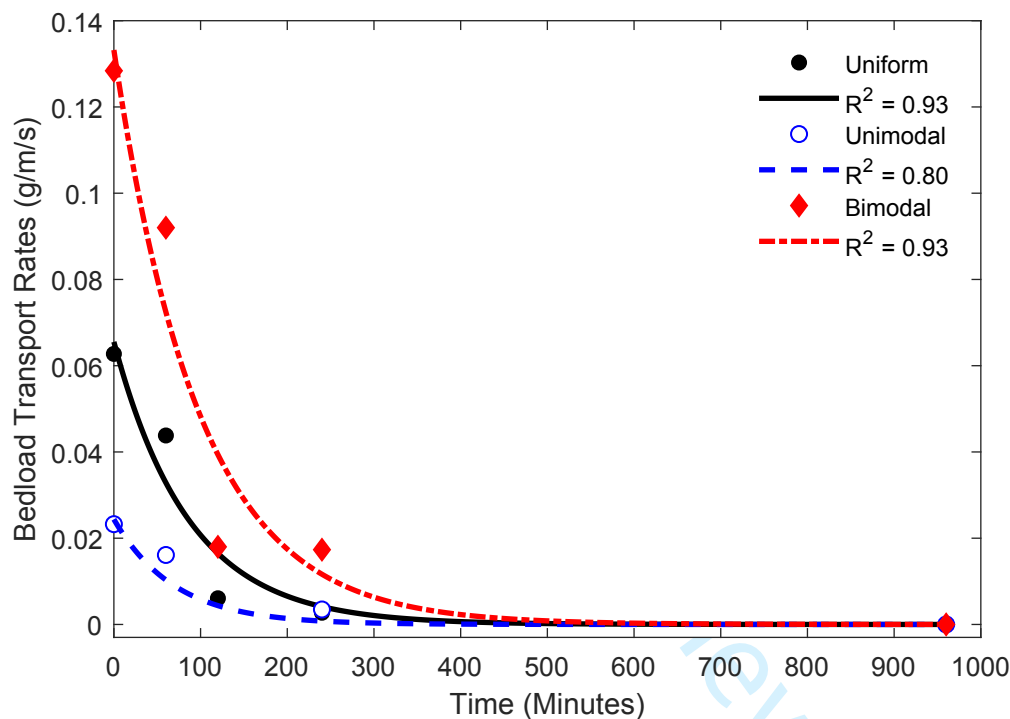


Figure 4: Inter-flood duration relationships with bedload transport rate, including the fitted exponential decay function of form $\Sigma Q_{bi} = \Sigma Q_{bi0} + (\Sigma Q_{bi\infty} - \Sigma Q_{bi0})e^{-kt}$ with R^2 values of 0.93, 0.80 and 0.93 for the uniform, unimodal and bimodal beds respectively.

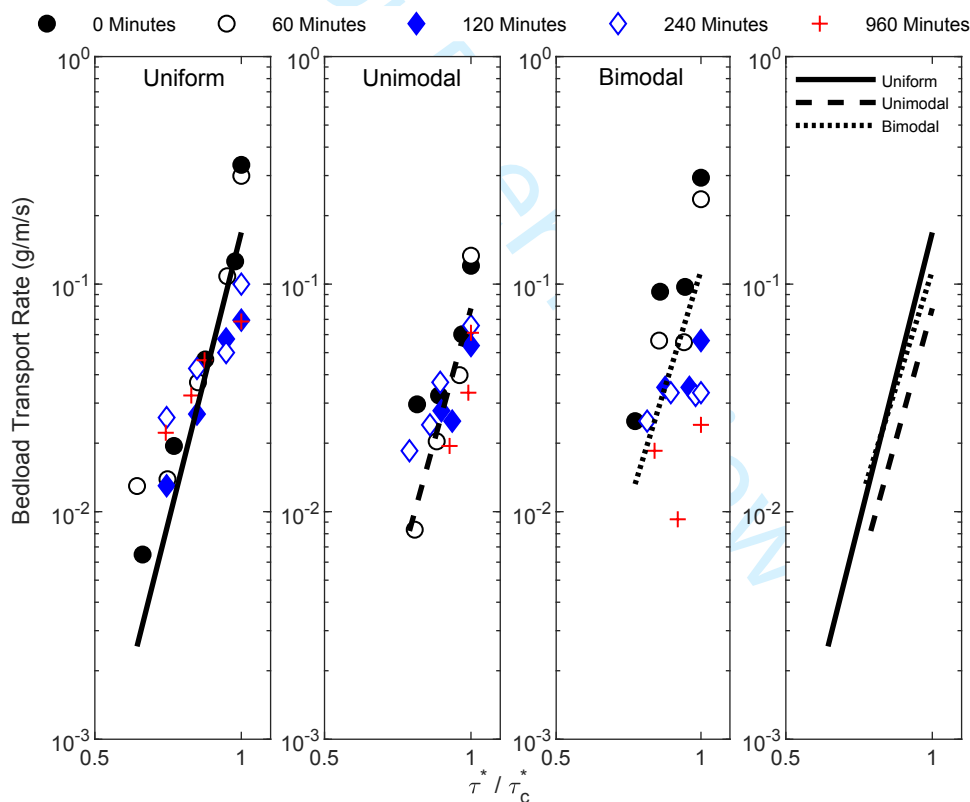
Following 960 minutes of antecedent conditioning, bedload transport rates were reduced by 91% for bimodal beds, 80% for near uniform beds, and 60% for unimodal beds (Figure 4, Table 4). The relationship between antecedent duration and bedload transport rate can be described by an exponential decay, however, akin to the entrainment threshold data, the rate of change is grade sensitive as indicated by the

1
2
3 365 half life value. The unimodal bed has the most rapid rate of decline with a half-life
4
5 366 time of approximately 48 minutes compared to the uniform and bimodal beds which
6
7 367 have half live times of 60 and 68 minutes respectively. Further, data indicates that
8
9 368 rate of reduction is linked with the predicted minimal transport rate value derived in
10
11 369 Table 4. Specifically, the unimodal bed decays the fastest but has a higher overall
12
13 370 predicted minimal transport rate as compared to the bimodal bed which decays over
14
15 371 the longest time period but decays to a lower minimal transport rate, as given in
16
17 372 Table 4.
18
19
20
21
22 373

23
24 374 In addition to reported relationships between inter-flood duration and bedload flux,
25
26 375 previous data has indicated that prolonged periods of sub threshold flow also have
27
28 376 the potential to delay to the onset of entrainment in the following flood (Reid and
29
30 377 Frostick, 1984). The first three subplots of Figure 5 plot $\frac{\tau^*}{\tau_c^*}$ at each step of the
31
32 378 stability test as a function of the bedload transport rate for the same step of the
33
34 379 stability test. The fitted trend line given in each of the subplots combines all of the
35
36 380 data for each bed and collapses them onto a single straight line using a least-square
37
38 381 error fitting approach; the power law fitted follows that of previous studies (Parker,
39
40 382 1990; Wilcock and Crowe, 2003; Recking 2010; Piedra, 2010) applicable to ranges
41
42 383 of $\frac{\tau^*}{\tau_c^*} < 1.3$. The final subplot of Figure 5 directly compares the trend lines derived for
43
44 384 each sediment bed.
45
46
47
48
49
50
51 385

52
53 386 For all three grain size distributions, there is the expected positive correlation
54
55 387 between dimensionless shear stress and total load such that increased time into the
56
57 388 stability test is correlated with an increase in transported load for each step of the
58
59
60

1
2
3 389 stability test. An inverse relationship is also noted between the antecedent duration
4
5 390 and transported load in each step of the stability test whereby a decrease in total
6
7 391 load is correlated to an increase in antecedent duration. Finally, there is an offset
8
9
10 392 noted on the abscissa in the two graded beds such that transport does not
11
12 393 commence until later in the stability test (i.e. at higher shear stresses) as antecedent
13
14 394 duration is increased; this is particularly noted within the bimodal bed. This suggests
15
16 395 that the mechanisms responsible for stabilising the bed are different between the
17
18 396 uniform and graded beds.
19
20
21
22 397



398

399 **Figure 5:** Relationship between $\frac{\tau^*}{\tau_c^*}$ at each step of the stability test as a function of
400 the bedload transport rate for the same step of the stability test for the uniform,
401 unimodal and bimodal beds respectively (subplots 1-3). The fitted trend line given in
402 each of the subplots combines all of the data for each bed and collapses them onto a
403 single straight line. The final subplot directly compares the trend lines derived for
404 each sediment bed. The exponent of the power law relationship is 11.06, 10.09 and
405 8.77 and the R_2 values of those fits are 0.63, 0.75 and 0.29 for the uniform, unimodal
406 and bimodal beds respectively.

1
2
3 407
4 408
5
6 409 When the data is scaled in terms of excess shear stress ($\frac{\tau^*}{\tau_c^*}$), the data appear to
7
8
9 410 collapse onto a single relationship. However, it is also clear that whilst the data
10
11 411 seems to more readily collapse for the uniform and unimodal beds the bimodal bed
12
13 412 exhibits significant scatter and the data derived from the longest inter-flood durations
14
15 413 (240 and 960 minutes) is not described well by the trend line.
16
17
18 414

19
20 415 Given the different rate and magnitude of response of the graded beds to increasing
21
22 416 inter-flood durations the following section uses fractional bedload transport patterns
23
24 417 to analyse the stability-mobility patterns of individual fractions within each bed in
25
26 418 order elucidate upon the underpinning bed stabilisation processes (Figure 6). Given
27
28 419 that the stability test was curtailed at the threshold for D_{50} , if size selective
29
30 420 entrainment is prominent no grains greater than the D_{50} should be moving ($g_i/F_i \neq 1$);
31
32 421 however, if grains greater than the D_{50} are moving then there is a tendency towards
33
34 422 equal mobility conditions ($g_i/F_i = 1$).
35
36
37
38 423

39
40
41 424 The unimodal bed is characterised by equal mobility conditions under 0 and 60
42
43 425 minutes of antecedent flow. However as antecedent duration is increased beyond
44
45 426 that the bedload response becomes more strongly size selective in the coarse and
46
47 427 fine end members of the distribution such that these grains stabilise and leave the
48
49 428 middle fractions of the transported distribution as being comparatively mobile. In
50
51 429 comparison, under benchmark conditions, the bimodal bed is characterised by equal
52
53 430 mobility particularly for in the grain fractions containing and surrounding the median
54
55 431 grain size. As antecedent duration is increased although size selective transport
56
57 432 conditions begin to develop in the finest members of distribution the degree of size
58
59
60

selectivity which develops is not as strong as that which develops in the unimodal bed.

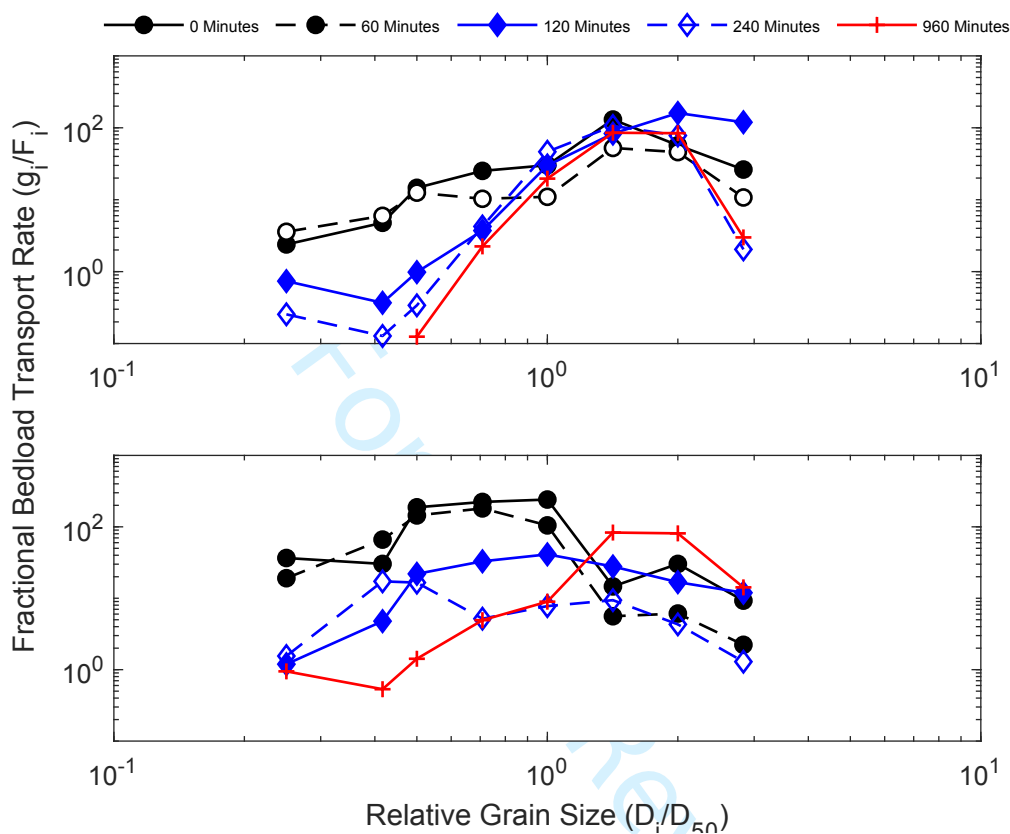


Figure 6: Fractional bedload transport rate of the unimodal (top plot) and bimodal bed (bottom plot) scaled by the abundance of each size (g_i) in the bulk mix (F_i) plotted against dimensionless grain size for antecedent durations 0-960mins. Given the stability test was stopped once the critical entrainment threshold of the D_{50} had been reached the data in this figure represent bedload which was collected during the last step of the stability test under these conditions.

4. DISCUSSION

4.1 Effect of inter-flood duration on bed stability

This paper has provided the first direct quantification of the response of different grain size distributions to inter-flood duration effects in terms of both entrainment threshold and bedload flux response. Analysis shows that all three grain size distributions responded to changes in antecedent duration. This is supportive of field

1
2
3 450 (e.g. Reid and Frostick, 1984; Reid *et al.*, 1985; Willetts *et al.*, 1987; Oldmeadow and
4
5 451 Church, 2006; Pfeiffer and Finnegan, 2018) and laboratory (Paphitis and Collins,
6
7 452 2005; Monteith and Pender, 2005; Haynes and Pender, 2007; Masteller and
8
9 453 Finnegan, 2016) data which have both indirectly and directly suggested that
10
11 454 antecedency may be an important control on entrainment thresholds and bedload
12
13 455 flux.
14
15
16
17 456

18
19 457 Critical shear stress of the median grain size increases by up to +18% after being
20
21 458 exposed 960 minutes of antecedent flow, with the uniform grain size distribution
22
23 459 being the most responsive and the unimodal least responsive. The changes to
24
25 460 entrainment threshold in this study are under half that noted by Paphitis and Collins
26
27 461 (2005) and Haynes and Pender (2007) who observed up to a 56% and 46% increase
28
29 462 in critical bed shear stress respectively. The sediment beds reported by Paphitis and
30
31 463 Collins (2005) were finer (0.19 to 0.77mm sand) and there were differences in the
32
33 464 bed preparation techniques between studies which is likely to explain the differences
34
35 465 in the observed results; screeded beds (this study; Church, 1978; Cooper and Tait,
36
37 466 2008) form more resistant initial structures than those formed under still water
38
39 467 conditions (Paphitis and Collins, 2005). Although Haynes and Pender (2007) used
40
41 468 the same bimodal mixture as this current paper the timescales were significantly
42
43 469 longer than those reported herein and they also used a discharge was above-
44
45 470 threshold for the D_{50} .
46
47
48
49
50
51 471

52
53 472 The changes to entrainment threshold have been linked with bed reorganisation
54
55 473 during the sub threshold flow period (Hassan and Church, 2000; Haynes and
56
57 474 Pender, 2007; Ockelford and Haynes, 2012; Masteller and Finnegan, 2016). Given
58
59
60

1
2
3 475 that the applied antecedent flow in this paper was set at τ_{c50}^* , active, large scale
4
5 476 processes of reorganisation as a result of grain entrainment are unlikely and thus
6
7 477 significant bed surface composition change should not occur (Sutherland, 1991;
8
9 478 Hassan and Church, 2000; Whiting and King, 2003). Instead inter-flood processes
10
11 479 appear to increase the importance of passive, grain scale processes which, in turn,
12
13 480 alter a beds resistance to entrainment via a change to surface texture (Dietrich *et al.*,
14
15 481 1989; Kirchner *et al.*, 1990; Fenton and Abbott, 1997; Schmeeckle and Nelson,
16
17 482 2003; Ockelford and Haynes, 2012). Specifically, Masteller and Finnegan (2016)
18
19 483 observe that the largest change in the bed surface elevation distribution occurs in the
20
21 484 tails of the distribution and this change is positively correlated to antecedent flow
22
23 485 duration. They attribute this to pivoting of unstable grains into more stable positions,
24
25 486 the filling of pockets left by displaced grains and the oscillation, reorientation and
26
27 487 reduced relative protrusion of grains which occur throughout the antecedent flow
28
29 488 period.
30
31
32
33
34
35
36
37

38 490 Results from this paper have also shown that grain size distribution is a key control
39
40 491 on the magnitude of response to inter-flood duration in terms of entrainment
41
42 492 threshold response; direct comparison shows uniform beds to be up to twice as
43
44 493 responsive as graded beds. Ockelford and Haynes, (2012) suggest the differences
45
46 494 in response between the uniform and graded beds is related to changes in bed
47
48 495 roughness which develop during the antecedent period. Using bed surface
49
50 496 topography data collected pre and post antecedent flows they observed a 12%
51
52 497 decrease in roughness of uniform beds as compared to a 15% and 40% increase in
53
54 498 roughness of unimodal and bimodal beds respectively. In the uniform bed the
55
56 499 decrease in bed roughness reduced the relative depth of localised pores and hence
57
58
59
60

1
2
3 500 reduced both the shear stress magnitude and variability across the bed surface (Li
4
5 501 and Komar, 1986; Kirchner *et al.*, 1990; Rollinson, 2006). Within the graded beds,
6
7 502 the magnitude of the inter-flood flow response is controlled by the rearrangement of
8
9 503 the bed which is permitted due the range of grain sizes. During the sub threshold
10
11 504 flows vertical winnowing of the finer grains serves to consolidate the framework
12
13 505 gravels and hence increase bed stability (Frostick *et al.*, 1984; Reid *et al.*, 1985;
14
15 506 Carling *et al.*, 1992; Allan and Frostick, 1999; Marion *et al.*, 2003; Ockelford and
16
17 507 Haynes, 2012).
18
19
20
21
22 508

23
24 509 However, data in this paper also indicates that the degree of response to increasing
25
26 510 inter-flood duration in graded beds is strongly linked to the percentage of fines in the
27
28 511 distribution such that the bimodal bed, which has the highest proportion of fines
29
30 512 (20% of the distribution between 1-2mm compared to 7.5% in the unimodal bed)
31
32 513 responds to a greater degree than the unimodal bed. It is thought that the process of
33
34 514 consolidation of the beds due to the infiltration of fines as described above drives this
35
36 515 response. This is in agreement with Cooper *et al.*, (2009), who assessed the
37
38 516 resistance to bedload transport of unimodal and bimodal deposits of similar D_{50} by
39
40 517 linking stability with the organisation of the surface deposits. Initially, their bimodal
41
42 518 beds had a higher degree of mobility due to a higher proportion of the fluid force
43
44 519 being carried by the finer grain fractions. However, as flow periods were increased,
45
46 520 a higher proportion of the fluid force was carried by the larger grains due to grain
47
48 521 sheltering (Schmeeckle and Nelson, 2003) and the development of grain structures
49
50 522 (Hassan and Church, 2000), such that the differences in the stability of the two beds
51
52 523 decreased.
53
54
55
56
57
58 524
59
60

1
2
3 525 The greatest rate of change in critical shear occurs for the shortest antecedent
4
5 526 durations which is in line with previous stress history research Paphitis and Collins,
6
7 527 2005; Monteith and Pender, 2005; Haynes and Pender, 2007; Ockelford and Haynes
8
9 528 2012; Masteller and Finnegan, 2016. However, interestingly the rate of change is
10
11 529 also grade specific where the unimodal bed responds to increasing inter-flood flow
12
13 530 duration is 2.5 times faster than the bimodal bed and 3 times as fast as the uniform
14
15 531 bed. Given the applied antecedent shear stress is set at τ_{c50}^* , it seems logical that
16
17 532 the uniform bed is less mobile under antecedent flows hence, it will take longer to
18
19 533 respond but once the bed has reorganised it will not be able to rearrange any further.
20
21 534 Within the graded beds the rearrangement processes responsible for stabilising the
22
23 535 bed will occur rapidly during the onset of the higher discharge conditions
24
25 536 experienced during the antecedent flow period but once the fines have winnowed
26
27 537 through the surface and consolidated the bed very little further rearrangement will
28
29 538 occur (Ockelford and Haynes 2012).
30
31
32
33
34
35
36
37

38 540 In relation to the bedload response to inter-flood duration up to a 91% reduction in
39
40 541 the bedload transport rate after 960 minutes of applied antecedent flow is observed.
41
42 542 Akin to the response of critical shear stress, the reduction in bedload transport rate
43
44 543 with increasing antecedent duration is nonlinear. This agrees with the previous
45
46 544 results of Haynes and Pender (2007) who also note an exponential decline in
47
48 545 transport rates as antecedent duration is increased. Whilst Masteller and Finnegan
49
50 546 (2016) fitted a linear model to their cumulative bedload flux data as a function of
51
52 547 increased conditioning flow, they do state that an exponential decline function also
53
54 548 fitted their data, albeit with lower model skill. Thus, these results are consistent with
55
56 549 an overall reduction in grain mobility, implying an increase in critical Shield's stress
57
58
59
60

1
2
3 550 with increased conditioning time. Such behaviour is similar to that of many
4
5 551 degradation experiments (Tait *et al.*, 1992; Proffitt and Sutherland, 1983; Pender *et*
6
7 552 *al.*, 2001). Haynes and Pender (2007) attributed this decay to the progressive
8
9 553 stabilisation of larger areas of the bed surface such that grains became unavailable
10
11 554 for transport. The decay to a constant flux even under the low shear stresses is
12
13 555 possible due to turbulent fluctuations in the flow (e.g. Grass, 1970; Paintal, 1971;
14
15 556 Graf and Pазis, 1977; Lavelle and Mofjeld, 1987; McEwan *et al.*, 2004; Paphitis and
16
17 557 Collins, 2005; Bottacin *et al.*, 2008) or to the fact that a population of high protruding
18
19 558 grains is always available for transport (Masteller and Finnegan, 2016).
20
21
22
23
24
25

26 560 There is an observable delay to the onset of entrainment in periods of unsteady flow
27
28 561 subsequent to sub threshold flow periods. During floods a hysteresis loops often
29
30 562 develop in sediment flux measurements, whereby different magnitudes of bedload
31
32 563 flux are produced on the rising and falling limbs of hydrographs for the same flow
33
34 564 magnitude (Reid *et al.*, 1985; Church *et al.*, 1998; Hassan *et al.*, 2006; Waters and
35
36 565 Curran, 2015; Mao, 2018). These studies have proved an intrinsic link between bed
37
38 566 structure characteristics and the total load transported (Reid *et al.*, 1985; Reid *et al.*,
39
40 567 1997), which serve to alter entrainment thresholds and hence bedload flux. Although
41
42 568 this paper has not run a full hydrograph after the sub threshold flow period, the
43
44 569 theoretical underpinnings behind the links between stability, surface structure and
45
46 570 sediment flux are transferable. This is evidenced by the fact that not only does the
47
48 571 data in this paper show a an offset in the initiation of motion, but that the total loads
49
50 572 are also be reduced for comparable shear stresses of the unsteady flow as sub
51
52 573 threshold flow duration is increased.
53
54
55
56
57
58
59
60

1
2
3 575 Although the bedload flux data appears to collapse readily for the uniform and
4
5 576 unimodal beds the bedload transport rates associated with the longest inter-flood
6
7 577 durations in the bimodal bed are not well described. This is supported by Piedra
8
9 578 (2010) who analysed five commonly employed sediment transport equations and
10
11 579 found that the rapid increase in transport rates with shear stress for approximately $\frac{\tau^*}{\tau_c^*}$
12
13
14
15
16 580 < 1.3 and the drastic reduction of the rate of increase of sediment transport rate at $\frac{\tau^*}{\tau_c^*}$
17
18
19 581 > 1.3 (Wiberg and Smith, 1989 Hassan and Woodsmith, 2004; Bathurst, 2007) did
20
21 582 not explain the relationships shown when sediment beds had been exposed to
22
23 583 prolonged periods of antecedent flow. Piedra related the deviation caused by the
24
25 584 effects of antecedent duration, as shown by the data herein, to stabilisation of the
26
27
28 585 bed surface and the delay to the onset of entrainment caused by bed surface
29
30 586 rearrangement. Neither factor are taken into account in commonly used transport
31
32 587 equations which derive critical entrainment thresholds purely based on bed grain
33
34
35 588 size distribution data and bed slope (Reid and Frostick, 1986; Gomez and Church,
36
37 589 1989; Wong 2003; Recking, 2010).

38
39 590
40
41
42 591 A change in the fractional transport rates following the antecedent conditioning
43
44 592 phase is reported. Typically, fractional bedload rates would tend towards moving
45
46 593 from size selective transport patterns under low shear stress, partial transport
47
48 594 conditions to equal mobility conditions under high shear stress, full mobility
49
50 595 conditions (Wilcock and McArdell, 1997; Shvidchenko and Pender, 2000). Since the
51
52 596 stability test in this paper was run until τ^*_{c50} it is assumed that the fractional mobility
53
54 597 patterns would be characterised by size selective entrainment owing to the partial
55
56 598 mobility conditions. This would be irrespective of the preceding applied antecedent
57
58 599 duration. In the unimodal bed there is a trend towards equal mobility in the

1
2
3 600 intermediary size fractions with selective entrainment of the end members of the
4
5 601 distribution (Ashworth and Ferguson, 1989; Wilcock and Southard, 1988; Kuhnle,
6
7 602 1992; Wilcock and McArdell, 1993; Laronne *et al.*, 1994). However as antecedent
8
9 603 duration is increased the bedload response becomes more strongly size selective in
10
11 604 the coarse and fine end members of the distribution; as this typically goes hand-in-
12
13 605 hand with an increase in grain hiding the effect is on mobility of the middle fractions
14
15 606 of the transported distribution (Brayshaw *et al.*, 1983; Li and Komar, 1986; Dietrich *et*
16
17 607 *al.*, 1989; Fenton and Abbott, 1997). Conversely in the bimodal bed, under
18
19 608 benchmark conditions, the bimodal bed is characterised by equal mobility particularly
20
21 609 for in the grain fractions containing and surrounding the median grain size. As
22
23 610 antecedent duration is increased, size selectivity begins to develop, particularly in
24
25 611 the finest members of distribution which appear to have stabilised on the bed
26
27 612 surface. This leaves the coarsest fractions to be over represented in the bedload.
28
29 613 This suggests that there are significant hiding effects which develop in response to
30
31 614 increasing inter-flood durations and underpin the theory that it is the relative size
32
33 615 effects which drive the response to inter-flood duration (Jackson and Beschta, 1984;
34
35 616 Ikeda and Iseya, 1988; Wilcock, 1988).
36
37
38
39
40
41
42
43
44
45

618 4.2 Implications

619 A number of important implications for river flows emerge from our results.
620 Increased bed stability in response to increased inter-flood duration manifests itself
621 via increased critical shear stress which may preclude reliable estimates of bedload
622 transport, as most predictive models reply on a specified critical shear stress (e.g.,
623 Meyer-Peter and Müller, 1948; Engelund and Fredsøe 1975; Wong and Parker,
624 2006). Despite numerous revisions to the Sheild's function, a single value of flow
60

1
2
3 625 intensity at particle entrainment is not just a disputed concept (Lavelle and Mofjeld,
4
5 626 1987) but its value has been shown to depend on a range of particle parameters
6
7
8 627 such as shape, size distribution and armouring (Parker et al., 1982; Carsons and
9
10 628 Griffiths, 1985; Carling et al., 1992; Buffington and Montgomery, 1997; Church et al.,
11
12 629 1998). These observations of an evolving, or history-dependent critical shear stress
13
14 630 which is related to grain size distribution makes the transition towards gravel bed
15
16 631 instability and active sediment transport difficult to predict and could form the basis
17
18 632 for incorporating an inter flood-duration 'correction factor' into existing entrainment
19
20 633 equations.
21
22
23
24 634

25
26 635 In order to correct for the effects of inter-flood flows entrainment thresholds need to
27
28 636 be based on experimental data derived from beds which have been exposed to
29
30 637 antecedent flows. The relationship between bedload transport rate and excess
31
32 638 shear stress used herein can be described by a power law similar with similar
33
34 639 exponent values to that used by previous authors (Parker, 1990; Wilcock and Crowe,
35
36 640 2003; Recking 2010; Piedra, 2011). However, as supported by Piedra (2011) data
37
38 641 in this paper also indicates that there is no unique equation with fixed parameters
39
40 642 capable of describing bedload transport behaviour for gravel channels which have
41
42 643 been exposed to differing inter-flood flow periods. Further, given changes in bed
43
44 644 stability in response to inter-flood flow duration are grade sensitive our results
45
46 645 indicate the not only is predicting entrainment based on a single critical Shields value
47
48 646 inaccurate but also that the D_{50} may not be the best grain fraction from which to
49
50 647 estimate entrainment thresholds (MacKenzie et al, 2018). This study has shown that
51
52 648 the finest and coarsest fractions are most responsive to inter-flood flow duration and
53
54 649 hence more realistic entrainment models might consider using these fractions to
55
56
57
58
59
60

1
2
3 650 define bed stability (Carling, 1987,1988; Ashworth and Ferguson,1989; Eaton and
4
5 651 Church, 2004; Tamminga et al., 2015; Eaton et al., 2015; MacKenzie and Eaton,
6
7 652 2017).

9
10 653
11
12 654 Increased pressure on water resources will require sophisticated environmental flow
13
14 655 guidelines to maintain habitat diversity, ensure ecosystem health and functioning,
15
16 656 and enable effective water resource management planning (Poff et al., 1997;
17
18 657 Tharme, 2003; 2010; Rolls & Arthington, 2014). Given managed flows are designed
19
20 658 to mimic natural flow regime and sediment dynamics, periods of prolonged low flow
21
22 659 prior to release will have a fundamentally different sediment transport response than
23
24 660 those with shorter low flow periods. Hence this research has significant implications
25
26 661 for the management and design of such flows (Lytle & Poff, 2004; Arthington et al.,
27
28 662 2006; Kiernan et al., 2012; Olden & Naiman, 2010; Poff and Schmidt, 2016).

29
30
31 663

32 33 34 35 664 **5. CONCLUSION**

36
37 665 Novel laboratory experiments in a recirculating flume have quantified the effects
38
39 666 between grain size distribution and inter-flood duration on gravel river bed stability.
40
41 667 Inter-flood duration effects have been shown to be ubiquitous regardless of surface
42
43 668 grain size distribution where direct entrainment threshold analysis shows that critical
44
45 669 shear stress of the median grain size increases by up +18% due to the applied inter-
46
47 670 flood duration of 960 minutes at τ_{c50}^* . The magnitude of response is contingent upon
48
49 671 grain size distribution; uniform beds are more responsive as compared to the graded
50
51 672 beds. The effects of inter-flood duration on entrainment thresholds can be well
52
53 673 predicted using models which both start and tend to finite values such that when $t =$
54
55 674 0 then $\tau_c = \tau_0$; when $t \rightarrow \infty$ then $\tau_c \rightarrow \tau_{max}$. Bedload transport rate has also been
56
57
58
59
60

1
2
3 675 shown to be responsive to inter-flood duration where up to a 91% reduction in
4
5 676 bedload was recorded for the longest antecedent flow periods. However, akin to the
6
7
8 677 entrainment threshold data there is also a grade dependent response which has
9
10 678 been attributed to the ability of the bed to rearrange into a more stable configuration
11
12 679 during the sub threshold flow periods. Changes in the transport pattern reflect this
13
14 680 stabilisation process where the percentage of fines within a distribution control the
15
16
17 681 extent to which equal mobility or size selective conditions are noted.
18
19
20 682

21 683 Results have implications for the prediction of entrainment thresholds, the accurate
22
23 684 prediction of bedload flux timing and magnitude and have implications for the
24
25 685 management of environmental flow design. However questions still remain as to
26
27 686 how antecedent shear stress magnitude may affect the stability gains and whether
28
29 687 there may be a threshold at which inter-flood flows may serve to destabilise the bed
30
31 688 surface. Further, an understanding of the interaction of the bed surface with the
32
33 689 overlying fluid flow regime with respect to the changes in the turbulent patterns
34
35 690 during inter-flood sub-threshold flows would also be a significant step forward in this
36
37
38 691 emerging research field.
39
40
41
42 692
43
44 693

46 694 **Acknowledgements**

47
48
49 695 *This research was funded by the Engineering and Physical Sciences Research*
50
51 696 *council (EPSRC) under grant code EP/EO30467/1 held by Haynes. The work was*
52
53 697 *undertaken at the School of Engineering, University of Glasgow and the authors*
54
55 698 *sincerely thank the technical staff for their assistance in this research. The authors*
56
57
58
59
60

1
2
3 699 *would like to thank the detailed reviewers comments received on the first draft of this*
4
5 700 *paper which have strengthened the paper greatly.*
6
7

8 701

9
10 702 **References**

11
12 703 Allan, A.F. and Frostick, L.E. 1999. Framework dilation, winnowing and matrix
13 704 particle size: the behaviour of some sand-gravel mixtures in a laboratory flume.
14 705 *Journal of Sedimentary Research* 69: 21–26
15 706

16 707 Arthington, A., Bunn, S., Poff, N., & Naiman, R. 2006. The Challenge of Providing
17 708 Environmental Flow Rules to Sustain River Ecosystems. *Ecological Applications* 16;
18 709 1311-1318.
19 710

20 711 Ashmore, P. 1988. Bedload transport in braided gravel-bed stream models. *Earth*
21 712 *Surface Processes and Forms* 13: 677-695.
22 713

23 714 Ashworth PJ, Ferguson RI. 1989. Size-selective entrainment of bed-load in gravel
24 715 bed streams. *Water Resources Research* 25: 627–634.
25 716

26 717 Bagnold, R. A. 1980. An empirical correlation of bedload transport rates in flumes
27 718 and natural rivers. *Proceedings of the Royal Society of London Series A* 372; 453-
28 719 473.
29 720

30 721 Barry, J. J., Buffington, J. M., Goodwin, P., King, J. G., and Emmett, W. W. 2008.
31 722 Performance of bed-load transport equations relative to geomorphic significance:
32 723 predicting effective discharge and its transport rate. *Journal of Hydraulic Engineering*
33 724 13: 601-615.
34 725

35 726 Bathurst, J.C. (2007). Effect of coarse surface layer on bedload transport. *Journal*
36 727 *of Hydraulic Engineering* 133: 1192-1205.
37 728

38 729 Bottacin-Busolin, A., Tait, S.J., Marion, A., Chegini, A., and Tregnaghi, M. 2008.
39 730 Probabilistic description of grain resistance from simultaneous flow field and grain
40 731 motion measurements. *Water Resources Research*. doi; 0.1090.2007WR006224
41 732

42 733 Buffington, J.M. and Montgomery, D.R. 1997. A systematic analysis of eight decades
43 734 of incipient motion studies, with special reference to gravel-bedded rivers. *Water*
44 735 *Resources Research*. 33; 1993–2029.
45 736

46 737 Carling P. 1987. Bed stability in gravel streams, with reference to stream regulation
47 738 and ecology. In *River Channels: Environmental and Process*, Richards K (eds),
48 739 *Institute of British Geographers Special Publications Series*, Wiley-Blackwell: Oxford;
49 740 321–347
50 741

51 742 Carling P. 1988. The concept of dominant discharge applied to two gravel-bed
52 743 streams in relation to channel stability thresholds. *Earth Surface Processes and*
53 744 *Landforms* 13: 355–367
54
55
56
57
58
59
60

- 1
2
3 745
4 746 Carling, P. A., A. Kelsey, and Glaister, M.S. 1992. Effect of bed roughness, particle
5 747 shape and orientation on initial motion criteria. In *Dynamics of Gravel-bed Rivers*.
6 748 Billi, P., Hey, R.D., Thorne, C.R. and Tacconi, P, (eds). Wiley; Chichester: 24–39
7 749
8 750 Carson, M.A. and Griffiths, G.A. 1987. Bedload Transport on gravel channels.
9 751 *Journal of Hydrology* 79; 375-378
10 752
11 753 Church, M. 1978. Palaeohydraulic Reconstructions From a Holocene Valley Fill. In:
12 754 *Fluvial Sedimentology*; Miall, A.D. (eds). Canadian Society of Petroleum Geologists.
13 755 Calgary. Canada. 743–772.
14 756
15 757 Church, M., Hassan, M.A. and Wolcott, J.F. 1998. Stabilizing self organized
16 758 structures in gravel-bed stream channels: Field and experimental observations.
17 759 *Water Resources Research* 34; 3169-3179.
18 760
19 761 Cooper, J.R. and Tait, S.J. 2008. Water worked gravel beds in laboratory flumes- a
20 762 natural analogue?. *Earth Surface Processes and Landforms* 34: 384-397.
21 763
22 764 Cooper, J.R. and Frostick, L.E. 2009. The difference in the evolution of the bed
23 765 surface topography of gravel and gravel-sand mixtures, 33rd IAHR Congress: Water
24 766 Engineering for a Sustainable Environment. International Association of Hydraulic
25 767 Engineering & Research. Vancouver, Canada.
26 768
27 769 Dietrich, W.E., Kirchner, J.W., Ikeda, H. and Iseya, F. 1989. Sediment supply and
28 770 the development of the coarse surface layer in gravel-bedded rivers. *Nature* 340;
29 771 215-217
30 772
31 773 Eaton, B.C. Church, M. 2004. A graded stream response relation for bed load-
32 774 dominated streams. *Journal of Geophysical Research* 109: F03011.
33 775 doi.org/10.1029/2003JF000062
34 776
35 777 Eaton B, MacKenzie, L., Jakob, M. and Weatherly, H. 2017. Assessing erosion
36 778 hazards due to floods on fans: Physical modelling and application to engineering
37 779 challenges. *Journal of Hydraulic Engineering* 143: 04017021.
38 780 doi.org/10.1061/(ASCE)HY.1943-7900.0001318
39 781
40 782 Engelund, F. And Fredsoe, J. 1976. A sediment transport model for straight alluvial
41 783 channels. *Hydrology Research* 7:293-306. doi.org/10.2166/nh.1976.0019
42 784
43 785 Fenton, J. D. and Abbott, J. E. 1977. Initial movement of grains on a stream bed: the
44 786 effect of relative protrusion. *Proceedings of the Royal Society of London*. 352; 523–
45 787 537
46 788
47 789 Frostick, L.E., Lucas, P.M. and Reid, I. 1984. The infiltration of fines into coarse-
48 790 grained alluvial sediments and its implications for stratigraphical interpretation.
49 791 *Journal of the Geological Society of London*. 141; 955-965.
50 792
51 793 Gomez, B. 1983. Temporal variations in the particle size distribution of the surficial
52 794 bed material: the effect of progressive armouring. *Geografiska Annaler*. 65; 183-192.

1
2
3
4
5
6
7
8
9
10
11
12
13
14
15
16
17
18
19
20
21
22
23
24
25
26
27
28
29
30
31
32
33
34
35
36
37
38
39
40
41
42
43
44
45
46
47
48
49
50
51
52
53
54
55
56
57
58
59
60

795

796 Gomez, B. And Church, M. 1989. An assessment of bed load sediment transport
797 formulae for gravel bed rivers. *Earth Surface Processes and Landforms* 25: 1116-
798 1186. doi.org/10.1029/WR025i006p01161

799

800 Graf, W.H. and Paxis, G.C. 1977. Deposition and erosion in an alluvial channel.
801 *Journal of Hydraulic Research*. 15; 151-166.

802

803 Grass, A.J. 1970. Initial instability of fine bed sand. *Journal of the Hydraulics*
804 *Division; American Society of Civil Engineering*. 96; 619-632

805

806 Hassan, M.A. and Church, M. 2000. Experiments on surface structure and partial
807 sediment transport on a gravel bed. *Water Resources Research*. 36; 1885-1895.

808

809 Hassan, M. A. and Woodsmith, R. D. 2004. Bed load transport in an obstruction-
810 formed pool in a forest, gravel bed stream. *Geomorphology* 58: 2003-221.

811

812 Hassan, M.A., Egozi, R., Parker, G., 2006. Experiments on the effect of hydrograph
813 characteristics on vertical grain sorting in gravel bed rivers. *Water Resources*
814 *Research*. doi.org/10.1029/2005WR004707.

815

816 Haynes, H. and Pender, G. 2007. Stress history effects on graded bed stability.
817 *Journal of Hydraulic Engineering* 33; 343-349.

818

819 Kiernan, J., Moyle, P. and Crain, P.K. 2012. Restoring native fish assemblages to a
820 regulated California stream using the natural flow regime concept. *Ecological*
821 *Applications*. 22: 1472-1482

822

823 Kirchner, J.W., Dietrich, W.W., Iseya, F. and Ikeda, H. 1990. The variability of critical
824 shear stress, friction angle, and grain protrusion in water-worked sediments.
825 *Sedimentology* 37; 647-672.

826

827 Krumbein, W. C. 1941. Measurement and geological significance of shape and
828 roundness of sedimentary particles. *Journal of Sedimentary Petrology* 1; 64-72.

829

830 Lavelle, W. and Mofjeld, H. O. 1987. Do critical stresses for incipient motion and
831 erosion really exist? *Journal of Hydraulic Engineering* 113: 370-388.

832

833 Li, Z. and Komar, P.D. 1986. Laboratory measurements of pivoting angles for
834 applications in selective entrainment of gravel in a current. *Sedimentology* 33; 5917-
835 5929.

836

837 Lytle, D.A. and Poff, N. 2004. Adaption to natural flow regimes. *Trends in Ecology*
838 *and Evolution*. 2: 94-100

839

840 MacKenzie, L.G., Eaton, B.C. and Church, M. 2018. Breaking from the average: Why
841 large grains matters in gravel bed streams. *Earth Surface Processes and Landforms*
842 DOI: 10.1002/esp.4465

843

- 1
2
3 844 MacKenzie LG, Eaton BC. 2017. Large grains matter: Contrasting bed stability and
4 845 morphodynamics during two nearly identical experiments. *Earth Surface Processes*
5 846 *and Landforms* 42: 1287–1295
6 847
- 7 848 Mao, L. 2018. The effects of flood history on sediment transport in gravel bed rivers.
8 849 *Geomorphology*. 322: 192 – 205. doi.org/10.1016/j.geomorph.2018.08.046
9 850
- 10 851 Marquis, G.A., Roy, A.G., 2012. Using multiple bed load measurements: toward the
11 852 identification of bed dilation and contraction in gravel-bed rivers. *Journal of*
12 853 *Geophysical Research*. 117, F01014. doi.org/10.1029/2011JF002120
13 854
- 14 855 Masteller, C.C. and Finnegan, N.J. 2017. Interplay between grain protrusion and
15 856 sediment entrainment in an experimental flume. *Journal of Geophysical Research:*
16 857 *Earth Surface* 122: 274-289 doi.org/10.1002/2017GL076747
17 858
- 18 859 Masteller, C.C., Finnegan, N.J., Turowski, J.M., Yager, E.M. and Rickermann, D.
19 860 2019. History dependent threshold for motion revealed by continuous bedload
20 861 transport measurements in a steep mountain stream. *Geophysical Research Letters*
21 862 46; 2583-2591
22 863
- 23 864 Marion, A., Tait, S.J. and McEwan, I.K. 2003. Analysis of small-scale gravel bed
24 865 topography during armouring. *Water Resources Research* 39; 1334-1345.
25 866
- 26 867 McEwen, I.K., Sorensen, M., Heald, J., Tait, S.J., Cunningham, G.J., Goring, D.G.
27 868 and Willetts, B.B. 2004. Probabilistic modeling of bed-load composition. *Journal of*
28 869 *Hydraulic Engineering*. 130; 129-139.
29 870
- 30 871 Meyer-Peter, E. and Müller, R. 1948. Formulas for bedload transport. *Proceedings of*
31 872 *the 2nd Meeting of the International Association for Hydraulic Research*, 3: 39–64.
32 873
- 33 874 Monteith, H. and Pender, G. 2005 Flume investigation into the influence of shear
34 875 stress history. *Water Resources Research* 41, doi:10.1029/2005WR004297.
35 876
- 36 877 Neill, C.R. and Yalin, M.S. 1969. Quantitative definition of bed movement. *Journal of*
37 878 *the Hydraulics Division, American Society of Civil Engineers* 95; 581-588.
38 879
- 39 880 Ockelford, A. And Haynes, H. 2012. The impact of stress history on bed structure.
40 881 *Earth Surface Processes and Landforms* DOI: 10.1002/esp.3348
41 882
- 42 883 Olden, J.D. and Naiman, R.J. 2009. Incorporating thermal regimes into
43 884 environmental flows assessments: modifying dam operations to restore freshwater
44 885 integrity. *Freshwater Biology*. 55: 86-107
45 886
- 46 887 Oldmeadow, D.F. and Church, M. 2006. A field experiment on streambed
47 888 stabilization by gravel structures. *Geomorphology* 78; 335–350.
48 889
- 49 890 Paintal, A.S. 1971. A stochastic model for bed load transport. *Journal of Hydraulic*
50 891 *Research*. 9; 527–553.
51 892
52
53
54
55
56
57
58
59
60

1
2
3
4
5
6
7
8
9
10
11
12
13
14
15
16
17
18
19
20
21
22
23
24
25
26
27
28
29
30
31
32
33
34
35
36
37
38
39
40
41
42
43
44
45
46
47
48
49
50
51
52
53
54
55
56
57
58
59
60

- 893 Paphitis, D. and Collins, M.B. 2005. Sand grain threshold, in relation to bed stress
894 history: an experimental study. *Sedimentology* 52; 827-838.
- 895
896 Parker, G. 1990. Surface-based bedload transport relation for gravel bed rivers.
897 *Journal of Hydraulic Research* 28: 417-436.
- 898
899 Parker, G., Dhamotharan, S., Stefan, H. 1982. Model experiments on mobile, paved
900 gravel bed streams. *Water Resources Research* 18: 1395-1408.
- 901
902 Pender, G., Hoey, T.B., Fuller, C. and Mcewan, I.K. 2001. Selective bedload
903 transport during the degradation of a well sorted graded sediment bed. *Journal of*
904 *Hydraulic Research* 39; 269-277.
- 905
906 Pfeiffer, A.M. and Finnegan, N.J. 2018. Regional variation in gravel riverbed mobility,
907 controlled by hydrologic regime and sediment supply. *Geophysical Research Letters*
908 45: 3097- 3106 doi.org/10.1002/2017GL076747
- 909
910 Piedra, M., (2010). Flume investigation of the effects of sub-threshold rising flows on
911 the entrainment of gravel beds. Unpublished Ph.D. Thesis. Department of Civil
912 Engineering. The University of Glasgow
- 913
914 Piedra, M. and Haynes, H. 2011. The spatial distribution of coarse surface grains
915 and the stability of gravel river beds. *Sedimentology* 59 (3); 1014-1029
- 916
917 Poff, N. L. and Schmidt, J. 2016. How dams can go with the flow. *Science*.
918 353:1099- 1100. DOI: 10.1126/science.aah4926
- 919
920 Poff, N.L., J.D. Allan, M.B. Bain, J.R. Karr, K.L. Prestegard, B.D. Richter, R.E.
921 Sparks, and J.C. Stromberg. 1997. The natural flow regime: a paradigm for river
922 conservation and restoration. *BioScience* 47:769-784.
- 923
924 Powell, D. M., Reid, I. and Laronne, J. B. 1999. Hydraulic interpretation of cross-
925 stream variations in bed-load transport. *Journal of Hydraulic Engineering* 125; 1243-
926 1252.
- 927
928 Powell, D. M., Reid, I. and Laronne, J. B. 2001. Evolution of bedload grain size
929 distribution with increasing flow strength and the effect of flow duration on the caliber
930 of bed load sediment yield in ephemeral gravel bed rivers. *Water Resources*
931 *Research* 37: 1463-1474.
- 932
933 Proffitt, G. T., and Sutherland, A. J. 1983. Transport of non uniform sediments.
934 *Journal of Hydraulic Research* 21; 33-43.
- 935
936 Recking, A. 2010. A comparison between flume and field bed load transport data
937 and consequences for surface-based bed load transport prediction. *Water*
938 *Resources Research* doi:10.1029/2009WR008007.
- 939
940 Recking, A., Liebault, F., Peteuil, C. and Joliment, T. 2012. Testing bedload transport
941 equations with consideration of time scales. *Earth Surface Processes and*
942 *Landforms*. 37: 774-789 doi.org/10.1002/esp.3213

1
2
3
4
5
6
7
8
9
10
11
12
13
14
15
16
17
18
19
20
21
22
23
24
25
26
27
28
29
30
31
32
33
34
35
36
37
38
39
40
41
42
43
44
45
46
47
48
49
50
51
52
53
54
55
56
57
58
59
60

943

Reid, I. and Frostick, L.E. 1984. Particle interaction and its effects on the thresholds of initial and final bedload motion in coarse alluvial channels. *Sedimentology of Gravels and Conglomerates*. In Koster, E.H and Steel, R.J.S. (eds). Canadian Society of Petroleum Geologists Memoir. 10: 61-68.

948

Reid, I., Frostick, L.E. and Layman, J.T. 1985. The incidence and nature of bedload transport during flood flows in coarse-grained alluvial channels. *Earth Surface Processes and Landforms* 10: 33-44.

952

Rollinson, G.K. 2006. Bed structure, pore spaces and turbulent flow over gravel beds. Unpublished Ph.D. Thesis. Department of Civil Engineering. The University of Hull.

956

Schmeeckle, M.W. and Nelson, J.M. 2003. Direct numerical simulation of bedload transport using a local, dynamic boundary condition. *Sedimentology* 50; 279-301.

960

Scheider, J., Rickermann, D., Turowski, J. and Kirchner, J. W. 2015. Self-adjustment of stream bed roughness and flow velocity in a steep mountain channel. *Water Resources Research*. 51: 7838-7859 doi.org/10.1002/esp.3213

964

Rolls, R.J, and Arthington, A.H. 2014. How do low magnitudes of hydrologic alteration impact riverine fish populations and assemblage characteristics? *Ecological Indicators*. 39:179–88.

968

Shaw, J. and Kellerhals, R. 1982. The composition of recent alluvial gravels in Alberta River beds. *Alberta Research Council Bulletin* 41; 151.

971

Shvidchenko, A.B., and Pender, G. 2000 Flume study of the effect of relative depth on the incipient motion of coarse uniform sediments. *Water Resources Research*. 36: 619 -628.

975

Sutherland, A. 1991. Hiding functions to predict self armouring. *Proceedings, International Grain Sorting Seminar*. ETH Zürich. 117; 273-298.

978

Tait, S.J., Willetts, B.B. and Maizels, J.K. 1992. Laboratory observations of bed armouring and changes in bedload composition. In *Dynamics of Gravel-bed Rivers*. Billi, P., Hey, R.D., Thorne, C.R. and Tacconi, P. (eds). Wiley; Chichester. 205-225.

982

Tamminga AD, Eaton BC, Hugenholtz CH. 2015. UAS-Based remote sensing of fluvial change following an extreme flood event. *Earth Surface Processes and Landforms* 40(11): 1464–1476.

986

Tharme, R.E. 2003. A global perspective on environmental flow assessment: emerging trends in the development and application of environmental flow methodologies for rivers. *River Research and Applications* 19: 397-442.

990

1
2
3
4
5
6
7
8
9
10
11
12
13
14
15
16
17
18
19
20
21
22
23
24
25
26
27
28
29
30
31
32
33
34
35
36
37
38
39
40
41
42
43
44
45
46
47
48
49
50
51
52
53
54
55
56
57
58
59
60

991 Waters, K.A., Curran, J.C., 2015. Linking bed morphology changes of two sediment
992 mixtures to sediment transport predictions in unsteady flows. *Water Resources*
993 *Research*. 51: 2724–2741. <https://doi.org/10.1002/2014WR016083>.

994
995 Whiting, P. and King, J. 2003. Surface particle sizes on armoured gravel
996 streambeds: Effects of supply and hydraulics. *Earth Surface Processes and*
997 *Landforms* 28:1459–1471.

998
999 Wiberg, P. L. and Smith, J. D. 1989. Model for calculating bedload transport of
1000 sediment. *Journal of Hydraulic Engineering* 1: 101-123.

1001
1002 Wilcock, P.R. 1993. Critical shear stress of natural sediments. *Journal of Hydraulic*
1003 *Engineering*. 119: 491-505.

1004
1005 Wilcock, P. R. and Crowe, J. C. 2003. Surface-based transport model for mixed-size
1006 sediment. *Journal of Hydraulic Engineering* 129: 120-128.

1007
1008 Wilcock, P. R. and McArdeell, B.W. 1997. Partial transport of a sand/gravel sediment.
1009 *Water Resources Research* 33; 235-245.

1010
1011 Willetts, B.B., Maizels, J.K. and Florence, J. 1987. The simulation of stream bed
1012 armouring and its consequences. *Proceedings of the Institute of Civil Engineering*.
1013 1; 799-814.

1014
1015 Wong, M. and Parker, G. 2006. Reanalysis and correction of bedload relation of
1016 MeyerPeter and Müller using their own database. *Journal of Hydraulic Engineering*
1017 132:1159–1168.

1018
1019 Zhang, X. and McConnachie, G. L. 1994. A reappraisal of the Engelud bed load
1020 equation. *Hydrological Sciences Journal* 39; 561-567.

Experiment Number	Distribution	Antecedent Flow Duration (Minutes)	Stability Test Duration (Minutes)	Critical Flow Depth (m)	Recorded Critical Dimensionless Shear Stress values	Average Critical Dimensionless Shear Stress
1,2,3,4	Near - Uniform	0	70	0.051 (0.025)	0.021, 0.019, 0.019	0.020 (0.013)
5,6,7,9		60	70	0.052	0.021, 0.02, 0.022	0.021
9,10,11,12		120	70	0.052	0.023, 0.021, 0.022	0.022
13,14,15,16		240	80	0.056	0.022, 0.021, 0.023	0.022
17,18,19,20		960	90	0.060	0.025, 0.022, 0.024	0.024
21,22,23,24	Unimodal	0	80	0.063 (0.032)	0.026, 0.024, 0.024	0.025 (0.010)
25,26,27,28		60	80	0.064	0.026, 0.025, 0.025	0.026
29,30,31,32		120	90	0.069	0.028, 0.027, 0.026	0.027
33,34,35,36		240	100	0.072	0.029, 0.028, 0.030	0.029
37,38,39,40		960	90	0.070	0.030, 0.029, 0.029	0.029
41,42,43,44	Bimodal	0	60	0.053 (0.030)	0.022, 0.019, 0.021	0.021 (0.012)
45,46,47,48		60	60	0.054	0.021, 0.02, 0.022	0.021
49,50,51,52		120	70	0.057	0.025, 0.021, 0.024	0.023
53,54,55,56		240	70	0.056	0.024, 0.022, 0.02	0.022
57,58,59,60		960	80	0.060	0.024, 0.025, 0.024	0.024

Table 1; Experimental information for all experiments detailing the length of the antecedent flow, the stability test duration, the critical flow depths and the recorded dimensionless shear stress values at the critical entrainment threshold for all experiments. Values in brackets for the critical flow depth represents the depth at $T^*_{C_{50}}$ i.e. the flow depth which was applied during the antecedent flow period. Values in brackets for the average critical dimensionless shear stress represent the $T^*_{C_{50}}$ values under benchmark conditions i.e. the shear stress which was applied during all of the antecedent flow periods calculated from where no antecedent flow is applied.

Bed Fit Parameters	Uniform	Unimodal	Bimodal
Maximal dimensionless shear stress	0.038	0.043	0.037
k (Minutes ⁻¹)	0.003	0.010	0.004
Time to half saturation (Minutes)	234	74	198
R^2	0.98	0.80	0.83
RMSE	0.0003	0.0013	0.0007
SSE	1.71e-07	1.59e-06	8.84e-07
% increase in dimensionless shear stress between 0-960 minutes	18	9	12
Predicted % increase in dimensionless shear stress between 0- and Max predicted	19	11	13

1043 **Table 2;** The parameters associated with the growth in shear stress over time
 1044 according Equation 2

Bed Fit Parameters	Uniform	Unimodal	Bimodal
Maximal dimensionless shear stress	0.040	0.044	0.037
Half Saturation Constant (Minutes)	285	84	214
R^2	0.98	0.71	0.82
RMSE	0.0004	0.0017	0.0011
SSE	5.15E-07	2.27E-06	9.54E-07
% increase in dimensionless shear stress between 0-960 minutes	18	9	12
Predicted % increase in dimensionless shear stress between 0 and Max predicted	24	11	13

1046 **Table 3;** The parameters associated with the growth in shear stress over time
 1047 according Equation 3.

1048
 1049
 1050
 1051
 1052
 1053
 1054
 1055

1056

Bed Fit Parameters	Uniform	Unimodal	Bimodal
Minimal Bedload Transport rate (g/m/s)	0.015	0.018	0.012
k (Minutes ⁻¹)	0.0115	0.0143	0.0102
Half Life (Minutes)	60.22	48.37	68.29
R ²	0.93	0.80	0.93
RMSE	0.009	0.006	0.017
SSE	2.38e-04	1.04e-04	8.96e-04

1057

1058

1059

1060

1061

Table 4; The parameters associated with the decay in bedload transport over time according to an exponential decay function

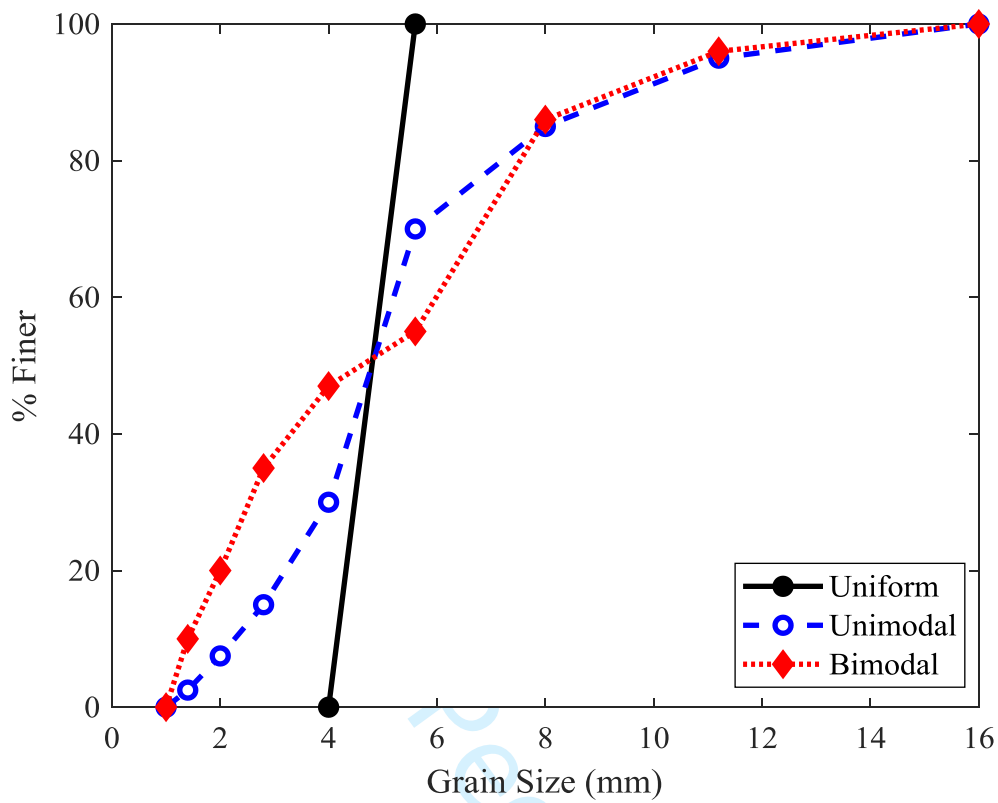


Figure 1: Grain size distribution for the three test sediment grades. The is calculated according to $\sigma_g = (D_{84}/D_{16})^{0.5}$

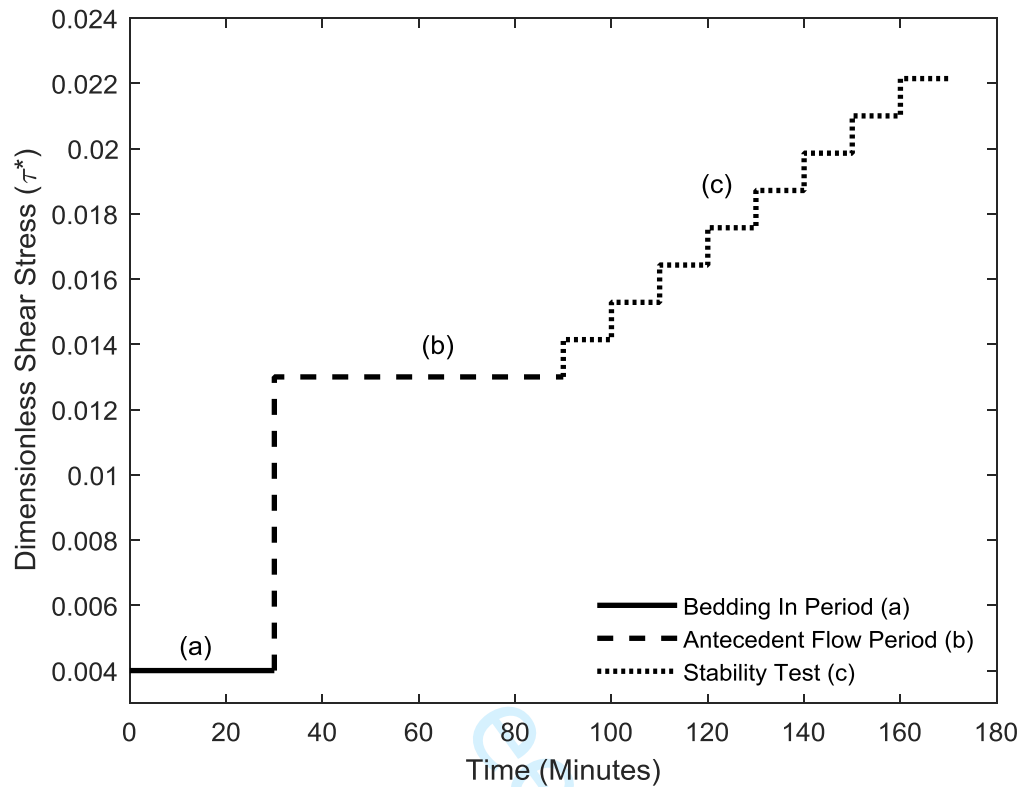


Figure 2: Sample experimental hydrograph detailing the three stages of the experiment: (a) an initial bedding in period run for 30 minutes at $\tau^* \sim 0.004$; (b) an antecedent flow period run at τ^*_{c50} for 0, 60, 120, 240 or 960 minutes; and (c) a stability test run until τ^*_{c50} is reached. The dimensionless shear stress values for each phase of each experiment are given in Table 1 with the example here given for the uniform bed exposed to 60 minutes of antecedent flow.

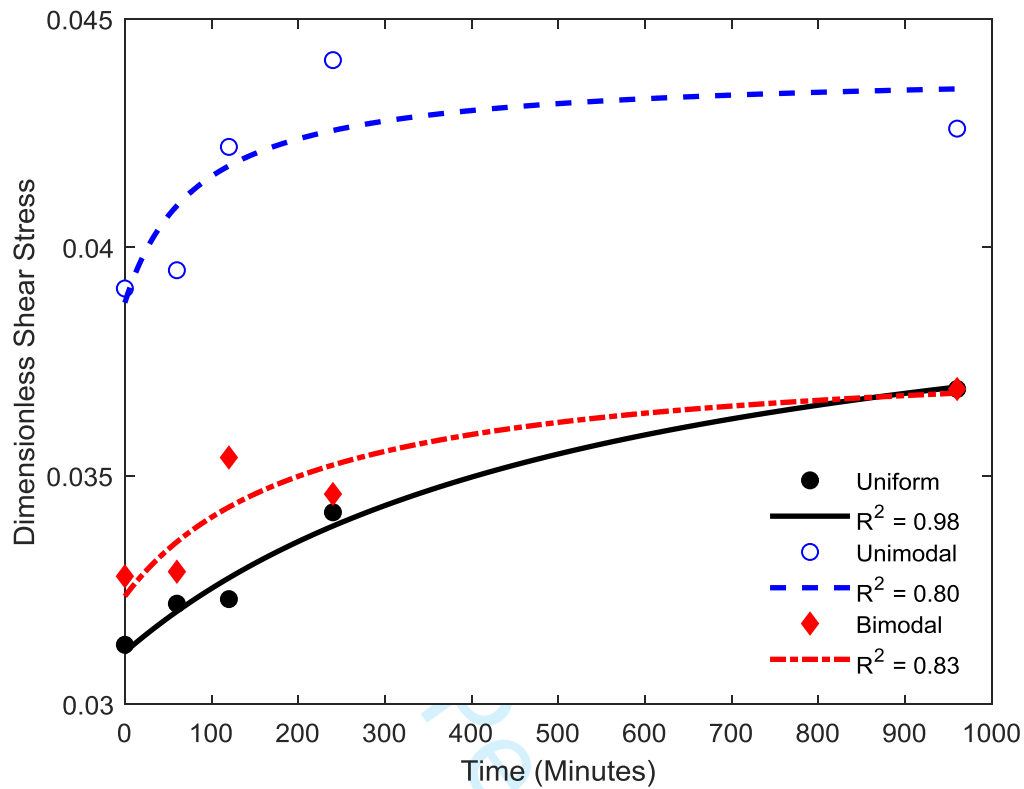


Figure 3: The relationship between antecedent duration, average critical dimensionless shear stress and grain size distribution with fits plotted derived according to Equation 2.

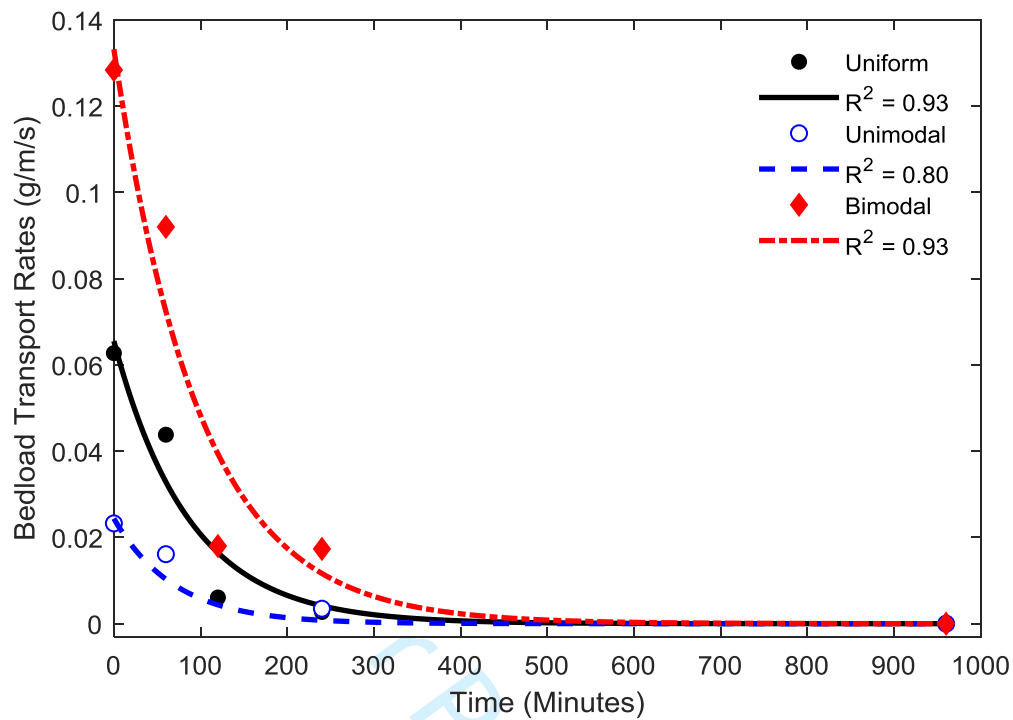


Figure 4: Inter-flood duration relationships with bedload transport rate, including the fitted exponential decay function of form $\Sigma Q_{bi} = \Sigma Q_{bi0} + (\Sigma Q_{bi\infty} - \Sigma Q_{bi0})e^{-kt}$ with R^2 values of 0.93, 0.80 and 0.93 for the uniform, unimodal and bimodal beds respectively.

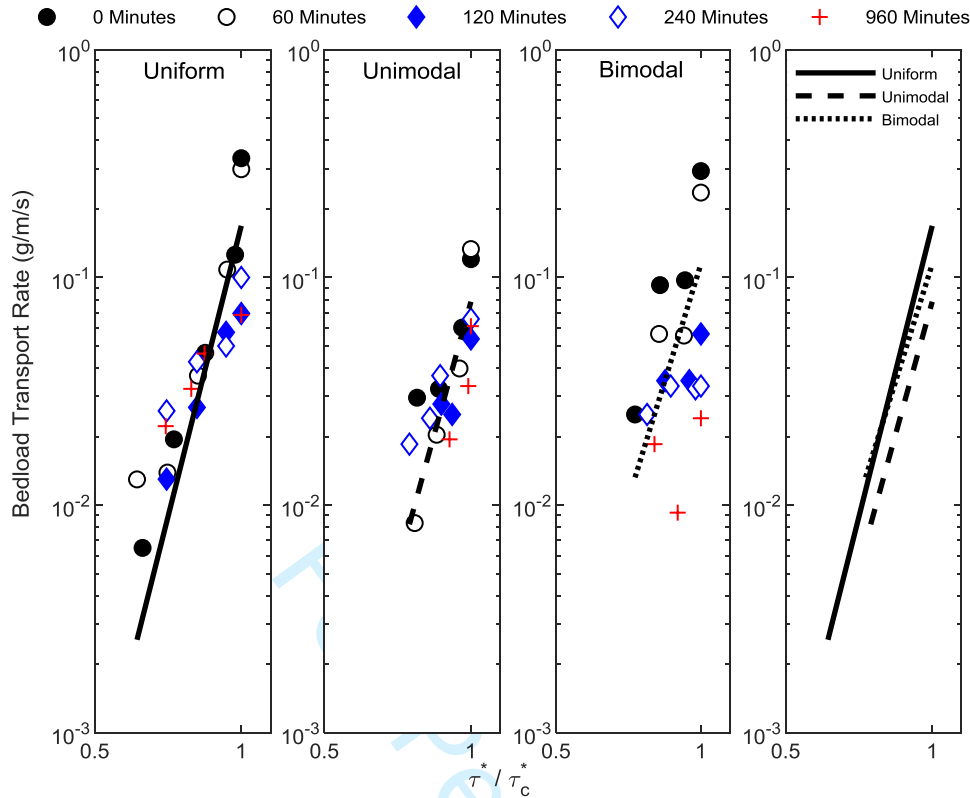


Figure 5: Relationship between $\frac{\tau^*}{\tau_c^*}$ at each step of the stability test as a function of the bedload transport rate for the same step of the stability test for the uniform, unimodal and bimodal beds respectively (subplots 1-3). The fitted trend line given in each of the subplots combines all of the data for each bed and collapses them onto a single straight line. The final subplot directly compares the trend lines derived for each sediment bed. The exponent of the power law relationship is 11.06, 10.09 and 8.77 and the R_2 values of those fits are 0.63, 0.75 and 0.29 for the uniform, unimodal and bimodal beds respectively.

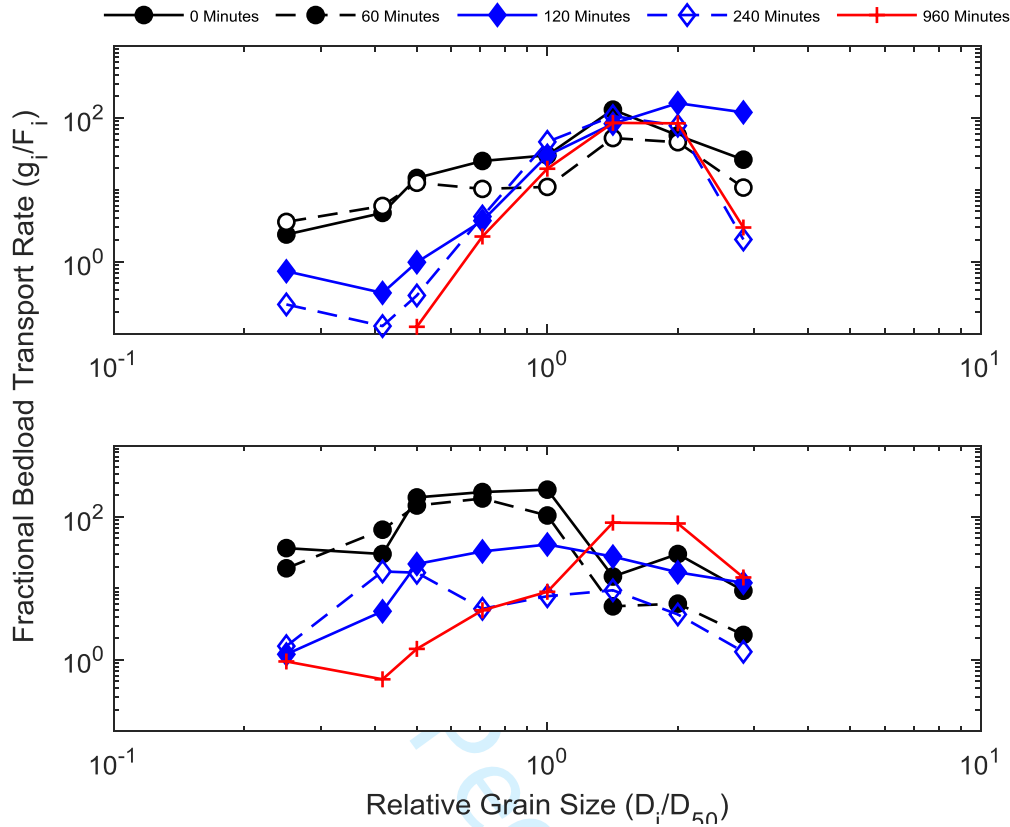


Figure 6: Fractional bedload transport rate of the unimodal (top plot) and bimodal bed (bottom plot) scaled by the abundance of each size (g_i) in the bulk mix (F_i) plotted against dimensionless grain size for antecedent durations 0-960mins. Given the stability test was stopped once the critical entrainment threshold of the D_{50} had been reached the data in this figure represent bedload which was collected during the last step of the stability test under these conditions.